# Simple formulation of no-cloning and no-hiding that admits efficient and robust verification

Matthew Girling [1,*] Cristina Cîrstoiu [2] and David Jennings [1,3]
[1] *School of Physics and Astronomy, University of Leeds, Leeds LS2 9JT, United Kingdom*
[2] *Quantinuum, 13-15 Hills Road, Cambridge CB2 1NL, United Kingdom*
[3] *Department of Physics, Imperial College London, London SW7 2AZ, United Kingdom*

(Received 30 May 2023; revised 23 January 2024; accepted 20 March 2024; published 24 April 2024)

Incompatibility is a feature of quantum theory that sets it apart from classical theory, and the inability to clone an unknown quantum state is one of the most fundamental instances. The no-hiding theorem is another such instance that arises in the context of the black-hole information paradox, and can be viewed as being dual to no-cloning. Here, we formulate both of these fundamental features of quantum theory in a single form that is amenable to efficient verification, and that is robust to errors arising in state preparation and measurements. We extend the notion of unitarity—an average figure of merit that for quantum theory captures the coherence of a quantum channel—to general physical theories. Then, we introduce the notion of compatible unitarity pair (CUP) sets, that correspond to the allowed values of unitarities for compatible channels in the theory. We show that a CUP set constitutes a simple "fingerprint" of a physical theory, and that incompatibility can be studied through them. We derive information-disturbance constraints on quantum CUP sets that encode both the no-cloning/broadcasting and no-hiding theorems of quantum theory. We then develop randomized benchmarking protocols that efficiently estimate quantum CUP sets and provide simulations using IBMQ of the simplest instance. Finally, we discuss ways in which CUP sets and quantum no-go theorems could provide additional information to benchmark quantum devices.

DOI: 10.1103/PhysRevResearch.6.023090

## I. INTRODUCTION

Quantum physics places much stronger limits on how we can transform information, compared to classical physics. These limits can be captured by the notion of incompatibility, that encapsulates fundamental impossibility results in quantum theory [1–4]. The most commonly encountered form of incompatibility refers to measurements—position and momentum cannot be simultaneously measured with the same precision—leading to formulations of no information without disturbance [5]. However, incompatibility can be described far more generally [6–8]. Two local processes on systems $A$ and $B$ are said to be compatible if there exists a *global* process that can produce both. The no-broadcasting theorem, an extension of the famous no-cloning theorem, can be cast as the incompatibility of local identity channels at $A$ and $B$ [4]. It is readily seen that if a physical theory admits perfect cloning, such as classical theory, then the theory cannot have any form of incompatibility.

Quantum technologies open new directions to experimentally test foundational aspects of quantum theory [9–13]. However, current devices are inherently noisy with error mitigation and correction being key obstacles to overcome for scalable quantum computing [14–17]. This presents a challenge in developing tests for foundational properties in a way that is robust to errors arising from the implementation of the experiment itself (e.g., at the state preparation and measurement stage). Viewed another way, such tests can also produce valuable benchmarks of errors in noisy intermediate scale quantum devices [18], as they have clear operational significance rooted in fundamental properties of quantum mechanics.

With this in mind, in this work we address the following question:

> *Can we formulate measures of quantum incompatibility that can be robustly and efficiently estimated?*

Existing criteria to decide the compatibility of quantum channels can be formulated generally in terms of semidefinite programming and by introducing witnesses of incompatibility [19,20]. The task has also been shown to be equivalent to the quantum state marginal problem [21]. Other formulations rely on the Fisher metric [22] or on the diamond norm [23] to capture information disturbance trade-offs. Another approach is via robustness measures [24,25]. Evaluating these different figures of merit for incompatibility requires extensive optimizations that typically assume access to a full description of the (quantum) processes involved.

The inability to clone a quantum state [1] can be shown to be an extremal case of incompatibility [6], and the ability to "hide" data in correlations can be viewed as being dual to cloning. This problem arises in the black-hole information

*m.j.girling@leeds.ac.uk

paradox [26–28], and the no-hiding theorem was established to prove the impossibility of hiding a qubit state in quantum correlations [26]. This has the implication that black hole information must have some degree of spatial localization, either within the black hole interior or in the external region to the black hole [26–28].

No-cloning and no-hiding can also be related to other quantum impossibility results such as no-masking [29,30] and no-deleting [31]. There have been some recent experimental tests of the no-hiding theorem [12] including the utilization of small scale quantum computers [32]. No-cloning has also been tested in the context of information disturbance [13]. However, here we develop a broader framework that exploits recent theoretical ideas that arise in the analysis of quantum technologies.

Our approach to this problem is motivated by randomized benchmarking techniques [33,34]. Such methods produce estimates of average channel properties (fidelity, unitarity etc.) in a way that is robust to state preparation and measurement (SPAM) errors and does not require exponentially difficult process tomography. In particular, we argue that the unitarity of a quantum channel, which is a measure of its coherence [35–37], is a natural means to *simultaneously* describe both no-cloning and no-hiding. In particular we show how such incompatibility can be captured by unitarity within a single information-disturbance inequality.

At a high level, our paper can be viewed as extending the simple concept of the purity of a state, which is a measure of disorder [38], to what can be viewed as a purity measure of the physical theory itself. This extension serves as a simple and intuitive two-dimensional "fingerprint" of the theory. An example for quantum theory is shown in Fig. 1.

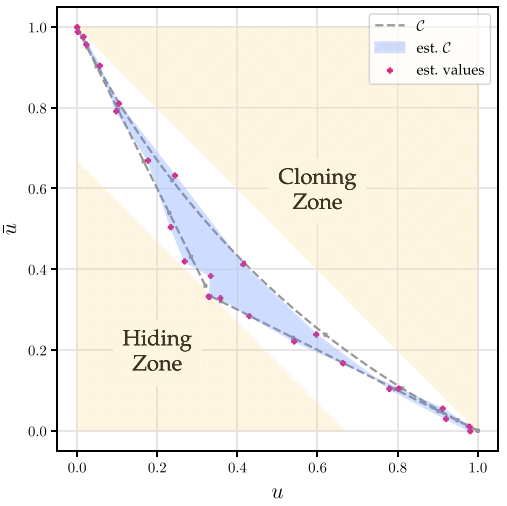


FIG. 1. Robust and efficient verification of quantum incompatibility. In classical theory we have the ability to perfectly clone and perfectly hide classical information. In contrast, quantum theory has fundamental incompatibility that prohibits the same behavior. This is captured by defining CUP sets, and shown here is the estimation of the simplest quantum CUP set $\mathcal{C}$. The reversible CUP set for classical theory corresponds to the full boundary of the unit square $[0, 1]^2$, and allows perfect cloning [the point (1,1)] and perfect hiding [the point (0,0)]. Using benchmarking techniques we estimate $\mathcal{C}$, shown here, on an IBM Q device and find that it saturates the general quantum bounds we derive in Theorem IV.1. Verifying such fundamental bounds provides a means to test the performance of emerging quantum computers.

### A. Structure and main results of the paper

Our main focus is to simultaneously handle both classical and quantum theories under a unifying umbrella using average channel properties. In Sec. II, we first develop a generalization of the *unitarity* $u(\mathcal{E})$ of a quantum channel, that allows extensions of our paper to more general physical theories [39–41]. We show that the unitarity has key properties that make it well suited to capturing compatibility, compared to other average measures such as fidelities [42,43].

We briefly summarize the framework we develop to capture incompatibility of a theory. For any theory and a globally isometric process $\mathcal{V}_{X\to AB}$ from a system $X$ into systems $AB$, we consider *marginal channels*

$$\mathcal{E} := tr_B \circ \mathcal{V}_{X\to AB}, \quad \bar{\mathcal{E}} := tr_A \circ \mathcal{V}_{X\to AB}, \tag{1}$$

by tracing out either $A$ or $B$ respectively. These channels let us define *compatible unitarity pairs* (CUPs), which we write as

$$(u(\mathcal{E}), u(\bar{\mathcal{E}})) \equiv (u, \bar{u}). \tag{2}$$

Ranging over the set of all valid CUPs in a probability theory forms a *CUP set* $\mathcal{C}$—which depends only on the underlying physical theory and the dimensions $d_X$, $d_A$, and $d_B$. In Sec. II, we show that CUP sets allow us to compare and contrast fundamental aspects of different physical theories, including incompatibility. In Sec. III, we establish that classical physics has a CUP set on the boundary of the unit square, while in stark contrast the simplest CUP set in quantum theory is described by a nontrivial shape in the plane (see Fig. 1).

We explain why the shape of CUP sets encode incompatibility and we prove (see Theorem IV.1) the following result:

**Result** (Incompatibility bound on quantum CUP set). *Any point* $(u, \bar{u})$ *in a quantum CUP set lies in the band defined by*

$$\frac{d_X}{d_X+1}\left(\frac{1}{d_A}+\frac{1}{d_B}\right) \leqslant u+\bar{u} \leqslant 1, \tag{3}$$

*where* $d_X$ *is the shared input system dimension, and* $d_A$ *and* $d_B$ *are the respective output dimensions.*

This provides a general constraint on any quantum CUP set. In Sec. IV, we relate this result to the no-cloning theorem and the impossibility of perfect hiding of quantum information under unitary evolution, to which there is no classical equivalent. Moreover, the above bounds are tight under general conditions that we discuss. Further, when $d_X = d_A = d_B$ a quantum CUP set captures the no-hiding theorem exactly (see Theorem IV.2), which we discuss in Sec. IV.

We next turn to the estimation of CUP sets on quantum devices. Firstly, by directly estimating a range of CUPs using the SWAP test [44]. These methods are detailed in Sec. V. Secondly, we consider how techniques for device benchmarking [35,45,46] can be used to estimate CUPs in a SPAM-robust way, see Secs. VI A and VI B. We show that—with some assumptions—quantum CUP sets can be estimated SPAM robustly on current devices (see Fig. 1).

Finally, we discuss how these methods compare, and to what degree we can infer that current devices obey the limits of quantum incompatibility.

## II. CUP SETS AND INCOMPATIBILITY

We now construct a framework to study fundamental incompatibilities of a physical theory in a form that is sufficiently simple to allow for efficient and robust estimation. The analysis in this section focusses on quantum and classical theory, but we can extend it to any general probabilistic theory as described in Appendix A.

### A. Unitarity of a general channel

We first introduce a measure—the unitarity—that quantifies how noisy a channel is. This measure can also be viewed as the variance of the channel [47]. For both quantum and classical theory, we have the notion of a physical state $x$ of a system, which may be mixed or pure [48]. For example, in classical statistical mechanics a pure state is a microstate, while a macrostate is a mixed state. The most general evolutions of states are called channels, and a channel $\mathcal{E}$, is simply any map that takes valid states to states. For example, the identity channel $id(x) := x$ for all states $x$. We next need a couple of additional concepts in order to define the unitarity of a channel.

Firstly, for both classical and quantum theory, we have a notion of geometry that arises for the states. In quantum theory we have the Hilbert-Schmidt inner product. For two Hermitian operators $A$ and $B$ this inner product is defined as $\langle A, B\rangle := \mathrm{tr}(AB)$, and leads to the definition of the *purity* of a quantum state $\rho$ given by $\gamma := \langle \rho, \rho\rangle = \mathrm{tr}(\rho^2)$. The same features exist in classical theory, and for a given probability distribution $(p_k)$ describing a classical state of a system we have its associated purity given by $\gamma(p) := \langle p, p\rangle := \sum_k p_k^2$. Therefore, in either classical or quantum theory, we can define the purity of a state $x$ as given by $\gamma(x) := \langle x, x\rangle$ for the appropriate inner product. The purity provides a measure of the noisiness of a given state, and for example can be associated to the minimal collision entropy over discriminating measurements in the theory [49]. Moreover, this quadratic-order measure can be readily estimated for either classical or quantum theory.

Secondly, for both quantum and classical theory we have a preferred measure $d\mu(x)$, which is nonzero over the set $\partial\mathcal{S}$ of pure states of the theory. For quantum theory this is the Haar measure, while for finite-dimensional classical systems it is the uniform measure over the discrete pure states.

Given this, we now define the *unitarity of a channel* $\mathcal{E}$ as

$$u(\mathcal{E}) := \mathrm{var}(\mathcal{E}) := \alpha \int_{\partial\mathcal{S}} d\mu(x)\, \gamma(\mathcal{E}(x-\eta)), \tag{4}$$

where $\eta := \int_{\partial\mathcal{S}} d\mu(x)\, x$ is the maximally mixed state under either quantum or classical theory, and where the normalizing constant $\alpha$ is chosen such that $u(id) = 1$.

This unitarity measure has a range of nice properties. For example, in Lemma A.1, we prove that $u(\mathcal{E}) = 0$ if and only if $\mathcal{E}$ is a completely depolarizing channel that acts as $\mathcal{E}(x) = y$ for all $x$ and some fixed $y$. Such a channel can be viewed as erasing all information in the input state of the system. Additionally, for any theory in which $\gamma(x) = \langle x, x\rangle$ the unitarity is bounded between 0 and 1, and $u(\mathcal{V}) = 1$ for all isometries $\mathcal{V}$ (see Corollary A.2), which are transformations that perfectly preserve all information in the input state $x$. Similarly, for such theories, the unitarity is invariant under changes of basis $u(\mathcal{V}_1 \circ \mathcal{E} \circ \mathcal{V}_2) = u(\mathcal{E})$ for any channel $\mathcal{E}$ and unitaries $\mathcal{V}_1, \mathcal{V}_2$ (see Lemma A.3) [35,50]. These attributes make unitarity a natural tool for capturing the incompatibility of channels.

### B. Defining cloning and hiding

Given a channel $\mathcal{G}$ from a subsystem $X$ to subsystems $AB$ we define the *marginal channels* as

$$\mathrm{tr}_B \circ \mathcal{G}(x), \tag{5}$$

$$\mathrm{tr}_A \circ \mathcal{G}(x), \tag{6}$$

where $\mathrm{tr}_A$ denotes the action of discarding the subsystem $A$, and similarly $\mathrm{tr}_B$ denotes discarding $B$. With the concept of a marginal channel, we can define what it means to clone or hide a state in a theory. The ability to perfectly clone/broadcast a state can be defined as the existence of a channel $\mathcal{G}$ from an input system $X$ to two output systems $A$ and $B$ such that

$$\mathrm{tr}_B(\mathcal{G}(x)) = id(x) = x, \tag{7}$$

$$\mathrm{tr}_A(\mathcal{G}(x)) = id(x) = x, \tag{8}$$

for all states $x$. In other words the state is perfectly copied to the two output subsystems. Note that broadcasting is where one allows correlations between the two output systems, while cloning does not have correlations and is normally considered for pure states only. This distinction is not important here since we focus on the marginal outputs only, and henceforth we refer to the above process as cloning. The no-cloning theorem [1] can therefore be cast as a statement that—under quantum theory—there is no channel $\mathcal{G}$ such that Eqs. (7) and (8) both hold for all states $x$.

The no-hiding theorem in its original formulation [26] says that given a quantum state $|\psi\rangle$ that unitarily evolves such that the output on one subsystem is a constant state—namely a completely depolarizing channel—then the state $|\psi\rangle$ can be perfectly recovered from the remaining environment subsystem. We can formulate the no-hiding theorem in terms of the above channel marginals in the following way. For a closed quantum system under unitary evolution (e.g., when $\mathcal{G} = \mathcal{V}$), if $\mathrm{tr}_B(\mathcal{V}(x)) = y$ for some fixed state $y$, then necessarily $x$ must be completely recoverable at $\mathrm{tr}_A(\mathcal{V}(x))$. Therefore the no-hiding theorem requires that $\mathrm{tr}_{B'} \circ \mathrm{tr}_A(\mathcal{V}(x)) = x$, up to final change of basis, and where the additional partial trace $(\mathrm{tr}_{B'})$ may be required to match the dimension of the input system.

Channel marginals can also capture a more general notion of hiding in any theory. More precisely, we say that we can perform *perfect* hiding in a theory if there is a channel $\mathcal{G}$ from an input system $X$ to two output systems $A$ and $B$ such that for all input states $x$ we have

$$\mathrm{tr}_B(\mathcal{G}(x)) = \mathcal{D}_1(x) = y_1, \tag{9}$$

$$\mathrm{tr}_A(\mathcal{G}(x)) = \mathcal{D}_2(x) = y_2, \tag{10}$$

where $\mathcal{D}_1$ and $\mathcal{D}_2$ are completely depolarizing channels send all states to the fixed states $y_1$ and $y_2$ respectively. In other words the marginal channels of $\mathcal{G}$ fully erase any information encoded in $x$. However, this is not everything. We also require that $x$ is genuinely encoded in the global correlations between $A$ and $B$. Therefore, we additionally require that $\mathcal{G}$ is a reversible transformation, which means there is another channel $\mathcal{F}$ from $A$ and $B$ to $X$ such that $\mathcal{F} \circ \mathcal{G}(x) = id(x) = x$. This defines perfect hiding, but it might be possible to have partial hiding of a state, in the same way as it is possible to partially clone a quantum state.

We next turn to quantifying how well a theory (classical, quantum, or a more general theory) can both clone and hide. To completely capture hiding our framework should reproduce both quantum theory's no-hiding theorem, as well as identify perfect hiding. We do this through the above focus on marginal channels, and use the unitarity to quantify how well these local channels preserve information.

### C. Compatible unitarity pairs of a theory

We now label the two marginal channels defined in Eq. (5) from the input system $X$ to the two output systems $A$ and $B$ as

$$\mathcal{E}(x) = \mathrm{tr}_B \circ \mathcal{G}(x), \tag{11}$$

$$\bar{\mathcal{E}}(x) = \mathrm{tr}_A \circ \mathcal{G}(x). \tag{12}$$

We name the tuple of the unitarities of these channels a *compatible unitarity pair* (CUP) and use the notation

$$(u(\mathcal{E}), u(\bar{\mathcal{E}})) \equiv (u, \bar{u}). \tag{13}$$

From the previous discussion of cloning and hiding we see that the set of global channels we consider $\mathcal{G}$ matters. For hiding, we must consider the set of isometric channels to capture quantum theory's no-hiding theorem—as well as the set of *reversible* channels for perfect hiding [51]. In contrast, for cloning we are free to range over all possible channels within a theory.

It is possible to describe a general process on a closed system in terms of reversible channels on (larger) open systems for both quantum and classical theory [52,53]. In quantum theory, global isometries suffice (captured by a Stinespring dilation [54]); however, classical theory requires the use of auxiliary randomness [53]. The *isometric channels* are a proper subset of reversible channels for both classical and quantum theory and are defined as those channels $\mathcal{V}$ for which we have $\langle \mathcal{V}(x), \mathcal{V}(y) \rangle = \langle x, y \rangle$ for all states $x, y$. The smaller set of isometry channels are the traditional set considered for incompatibility in quantum theory, due to the Stinespring dilation theorem.

When $\mathcal{G} \in \mathcal{V}$, the set of isometric channels, and $\mathcal{E}$ and $\bar{\mathcal{E}}$ are its marginal channels [as defined in Eqs. (11) and (12)] then we write $\mathcal{E} \sim \bar{\mathcal{E}}$ and say that these channels are isometrically compatible. In this case, for quantum theory, the channels $\mathcal{E}$ and $\bar{\mathcal{E}}$ are complementary to each other.

Similarly if $\mathcal{G} \in \mathcal{R}$, the set of reversible channels, then we write $\mathcal{E} \sim_r \bar{\mathcal{E}}$. Finally, when we consider $\mathcal{G}$ to be the set of *all* channels in a theory, we write $\mathcal{E} \sim_* \bar{\mathcal{E}}$ such that $\mathcal{E}$ and $\bar{\mathcal{E}}$ are marginals of any valid channel $\mathcal{G}$ from $X$ to $AB$. This notation is just to simplify definitions, and does not suggest an equivalence relation.

We now define the *set* of *compatible unitarity pairs* (the CUP set) as

$$\mathcal{C}^{X\to AB} := \{(u(\mathcal{E}), u(\bar{\mathcal{E}})) \in \mathbb{R}^2 : \mathcal{E} \sim \bar{\mathcal{E}}\}, \tag{14}$$

which is determined by both the structure of the particular state spaces and the admissible isometry channels in the theory. In a similar way, we define the *reversible CUP set*, $\mathcal{C}_r^{X\to AB}$, when $\mathcal{E} \sim_r \bar{\mathcal{E}}$. Finally, we define the *full CUP set* $\mathcal{C}_*^{X\to AB}$ for the marginals of any valid channel, when $\mathcal{E} \sim_* \bar{\mathcal{E}}$.

For the remainder of this paper we shall drop the superscripts specifying the subsystems and just write $\mathcal{C}$, $\mathcal{C}_r$, and $\mathcal{C}_*$ for the CUP sets.

Since the unitarity is bounded between 0 and 1, we have the following series of inclusions:

$$\mathcal{C} \subseteq \mathcal{C}_r \subseteq \mathcal{C}_* \subseteq [0, 1]^2. \tag{15}$$

It turns out that CUP sets can be defined for general probabilistic theories, and we discuss this in Appendix A. Note that for any theory we have $(0, 0) \in \mathcal{C}_*$, since we are always free to discard the input state and prepare an arbitrary constant state on the output systems (for which the unitarity vanishes). Likewise, since the identity channel is in any theory, and we are free to swap/relabel subsystems (all isometric processes) we also have that (1,0) and (0,1) lie in $\mathcal{C}$. These are common points for CUP sets across different physical theories.

### D. No-cloning and no-hiding through the CUP set

No-cloning and no-hiding fit into this framework as follows. Firstly, if the physical theory admits perfect cloning then this implies that $(1, 1) \in \mathcal{C}_*$ since $u(\mathcal{E}) = 1$ if and only if $\mathcal{E} = id$ up to a final isometry [50]. We also note that it has been shown [3,39] that broadcasting is possible in a physical theory if and only if the theory has a simplex state space of perfectly distinguishable states, and so essentially only classical theory has (1,1) in its CUP sets. The no-cloning theorem can be cast compactly as a statement that—for quantum theory, the full CUP sets $\mathcal{C}_*$ (and therefore all CUP sets) exclude the point (1,1).

Secondly, from Sec. II B, the no-hiding theorem given in terms of marginal channels states that—for quantum theory under isometric evolution—if $\mathcal{E} = \mathcal{D}$ (a completely depolarizing channel) then necessarily the input state can be completely recovered in the other subsystem. In the case $d_X = d_A = d_B$, this implies $\bar{\mathcal{E}} = \mathcal{V}$, an isometry. We will show (see Sec. IV) that this statement of the no-hiding theorem is captured exactly by the isometric quantum CUP set $\mathcal{C}$, as for the point $(0, x)$ in $\mathcal{C}$ then $x = 1$ only. Additionally in the case of unequal subsystems, the no-hiding theorem and the impossibility of perfect hiding implies the point (0,0) must still be strictly excluded from the isometric CUP set $\mathcal{C}$. We prove this also holds in Sec. IV.

We also consider whether a theory admits perfect hiding with the addition of auxiliary randomness. This is captured by the reversible CUP sets $\mathcal{C}_r$. If the theory admits perfect hiding with auxiliary randomness then we have $\mathcal{D}_1 \sim_r \mathcal{D}_2$ for some completely depolarizing channels $\mathcal{D}_1$ and $\mathcal{D}_2$. However, as we prove in the Appendices, this statement is equivalent to the

existence of the origin in the reversible CUP set, $(0,0) \in \mathcal{C}_r$. We will show that the reversible CUP sets of classical probability theory always contain (0,0) whereas the quantum reversible CUP sets only contain (0,0) under certain dimensional restrictions related to mixed state purification.

Finally, for both quantum and classical theory we examine the case with the smallest nontrivial dimensions in detail. Since quantum physics neither admits perfect cloning, nor perfect hiding under unitary evolution, the simplest quantum CUP sets form nontrivial subsets of the unit square $[0,1]^2$, which we discuss shortly. In contrast, both (0,0) and (1,1) always lie within the classical (reversible) CUP sets.

## III. CLASSICAL CUP SETS

We now explore in detail how the classical CUP set captures the compatibility allowed in classical probability theory. We shall see that the CUP sets of classical theory are radically different from quantum theory, and so are a simple and vivid way to contrast the two theories.

### A. Unitarity of classical channels

For a classical probability distribution on a $d$-dimensional system, the pure states correspond exactly to the $d$ extremal points $\{x_i\}_{i=1}^{d}$ of the state space. The unitarity reduces to

$$u(\mathcal{E}) = \frac{d}{d-1}\sum_{i=0}^{d-1}\gamma(\mathcal{E}(x_i-\eta)), \tag{16}$$

where $\eta = \frac{1}{d}\sum_{i=0}^{d-1} x_i$ is the maximally mixed state.

The only isometric operations with input and output systems of the same dimensions are those that permute the pure states. Recall that for any isometry we have $u = 1$. Furthermore, reversible classical channels are fully generated by the set of isometries and auxiliary classical randomness [53,55,56], as they correspond to injective Boolean functions. This allows us to characterize CUP sets for classical theory.

The state space of a single probabilistic classical bit is a $d = 2$ system with two possible pure states $x_0 := (1,0)$ and $x_1 := (0,1)$ in $\mathbb{R}^2$. Any pure state $x_m$ encodes the bit $m \in \{0,1\}$. There are only two single-bit isometries: the identity channel $id$ and NOT operation for which $\mathrm{NOT}(x_0) = x_1$ and $\mathrm{NOT}(x_1) = x_0$. For a two-bit system $d = 4$, we can define the pure states through the tensor product of the single bit pure states, e.g., $x_{ab} := x_a \otimes x_b$ for $a, b \in \{0,1\}$.

### B. Cloning and hiding in classical theory

To clone/broadcast a classical probabilistic bit in a state $x := (p, 1-p)$ with $0 \leqslant p \leqslant 1$, one simply brings in an auxiliary bit in the pure state $x_0 = (1,0)$ and then performs a controlled-not (CNOT) gate, controlled on the state $x$ with the auxiliary bit as the target. The marginal distributions are then both given by $x$; the input information was perfectly copied to the marginals. In terms of channels, the protocol is simply given by

$$\mathcal{V}_{\mathrm{broad}}(x) = \mathrm{CNOT}(x \otimes x_0), \tag{17}$$

which outputs a 2-bit state.

Hiding of a deterministic bit involves encoding a bit $m = 0$ or $m = 1$ entirely in correlations so that the marginal bit states are $\eta = (1/2, 1/2)$, the maximally disordered state. However, we also require that the bit $m$ is still perfectly recoverable from the total state. This can be done as follows, using the general case of a probabilistic bit state, $x := (p, 1-p)$. We introduce a single auxiliary bit in the state $\eta$, which is viewed as an unknown key bit, and we perform a controlled-not gate on $x$ that is controlled on $\eta$. Equivalently we get

$$\mathcal{R}_{\mathrm{hide},1/2}(x) = \mathrm{CNOT}(\eta \otimes x), \tag{18}$$

which is a correlated 2-bit state. It has marginals $\eta$ but since $\mathrm{CNOT} \circ \mathrm{CNOT} = id$ we can perfectly recover $x$ from the joint 2-bit state. This is the classical one-time-pad protocol for encryption and the operation performs perfect hiding in classical theory [57].

### C. The simplest classical CUP set

The most general isometries from a single bit into two bits take the form of $\mathcal{V}(x) := \pi_{AB}(x \otimes x_0)$ where $\pi_{AB}$ is a permutation on the four basis states. There will be six such different isometric operations; however, they produce the same three points on the CUP diagram as follows. As the unitarity of the marginal channels $\mathcal{E}$ and $\bar{\mathcal{E}}$ are invariant under local isometries at $A$ and $B$, then separable operations $\pi_{AB} = \pi_A \otimes \pi_B$ will give the point $(u, \bar{u}) = (1,0)$, corresponding to $\mathcal{E} = id$ and $\bar{\mathcal{E}} = \mathcal{D}$. The swap operation permuting the two systems will produce the point $(u, \bar{u}) = (0,1)$. Finally, if the permutation corresponds to the CNOT operation with control on system $A$, then on the CUP set diagram this gives the point $(u, \bar{u}) = (1,1)$, as $\mathcal{E} = \bar{\mathcal{E}} = id$. We therefore have that

$$\mathcal{C} = \{(1,0), (0,1), \text{ and } (1,1)\}, \tag{19}$$

for the simplest nontrivial CUP set in classical theory.

### D. Classical reversible CUP set

We now consider the CUP set produced by the set of reversible global operations $\mathcal{R}$.

The following class of operations

$$\mathcal{R}_p(x) = x \otimes (px_0 + (1-p)x_1) \tag{20}$$

introduces an auxiliary system $B$ prepared in a fixed probabilistic state. This is not isometric, but satisfies $tr_B \circ \mathcal{R}_p(x) = x$, and is therefore reversible. All such channels $\mathcal{R}_p$ correspond to point $(u, \bar{u}) = (1,0)$ of the CUP sets. Generally, reversible operations are given by

$$\mathcal{R} := \pi_{AB} \circ \mathcal{R}_p. \tag{21}$$

Motivated by the single-bit hiding protocol in Sec. III B, we consider $\pi_{AB} = \mathrm{CNOT}_{AB}$, the controlled-not with $A$ as the control and with $B$ as the target, that generates the following family of reversible maps

$$\mathcal{R}_{\mathrm{hide,p}} := \mathrm{CNOT}_{AB} \circ \mathcal{R}_p. \tag{22}$$

These are partially hiding channels with the perfect-hiding channel occurring for $p = 1/2$, corresponding to the point $(u, \bar{u}) = (0,0)$. For general $p \in [0,1]$ we have $(u, \bar{u}) = (1, p')$ with $p' = (1-2p)^2$. Since we can swap output subsystems

we also get $(u, \bar{u}) = (p', 1)$. The remaining reversible channels are obtained from

$$\mathcal{R}_{\text{broad},p} := \text{CNOT}_{BA} \circ \mathcal{R}_p, \tag{23}$$

which gives the points $(u, \bar{u}) = (0, p')$ with $p' = (1-2p)^2$ and similarly, $(u, \bar{u}) = (p', 0)$ if we swap the output subsystems. We therefore have that

$$\mathcal{C}_r = \{(t, 0), (0, t), (t, 1), \text{ and } (1, t) \text{ for all } t \in [0, 1]\}. \tag{24}$$

In other words the reversible CUP set $\mathcal{C}_r$ is simply the border of the unit square $[0, 1]^2$.

### E. Classical full CUP set

Finally, we consider the full 1 to 2 bit CUP set $\mathcal{C}_*$ obtained by ranging over all single-bit to two-bit systems. It can be shown (see Corollary A.1) that if a global channel $\mathcal{E}$ from $X$ to $AB$ gives a point $(u, \bar{u})$ in any CUP set and $\mathcal{D}$ is any global, completely depolarizing channel, then the set of convex mixtures $p\mathcal{E} + (1-p)\mathcal{D}$ give the line segment joining $(u, \bar{u})$ to (0,0). This automatically implies that for classical theory we have

$$\mathcal{C}_* = [0, 1]^2, \tag{25}$$

since we can take convex mixtures of reversible channels with a completely depolarizing channel and the resulting line segments fill the unit square.

## IV. QUANTUM CUP SETS

Quantum CUP sets are much more tightly constrained in the unit square $[0, 1]^2$ than their classical counterparts, and we relate this to quantum no-go theorems. In this section we provide evidence for this statement, via tight analytical bounds on the sum of quantum CUPs.

### A. Unitarity of quantum channels

Under quantum theory, from Eq. (4), the unitarity of a quantum channel $\mathcal{E} : \mathcal{B}(\mathcal{H}_X) \to \mathcal{B}(\mathcal{H}_Y)$ is

$$u(\mathcal{E}) := \frac{d_X}{d_X - 1} \int d\psi \, \text{tr}[\mathcal{E}\left(\psi - \frac{\mathbb{1}_X}{d_X}\right)^2], \tag{26}$$

where $d_X$ is the dimension of system $X$, and where the integration is with respect to the Haar measure.

Within the context of benchmarking quantum devices, the unitarity $u$ of the average noise channel $\mathcal{E}$ associated with a gateset can be estimated using randomized benchmarking (RB) [58]. The unitarity of a noise channel gives additional information, beyond the average gate fidelity [37]. Knowing the unitarity of a channel in addition to the average gate fidelity, gives improved bounds on the diamond norm distance of a given channel to the identity [59], a key figure of merit for fault-tolerant computation. Benchmarking protocols to estimate the unitarity of noise are efficient and robust against state preparation and measurement (SPAM) errors.

### B. Incompatibility and hiding via trade-off relations on CUP sets

We can now establish the following general bounds on the quantum CUP sets that arise from isometric channels. This gives us a handle on the structure of such sets and in particular how they relate to cloning and hiding.

*Theorem IV.1 (General bounds on quantum CUP set $\mathcal{C}$).* Given any input system $X$ of dimension $d_X$ and output systems $A$ and $B$ of dimensions $d_A, d_B$, with $d_X \leqslant d_A d_B$. The associated quantum CUP set $\mathcal{C} \subseteq [0, 1]^2$ is confined to the band in the $(u, \bar{u})$ plane defined by

$$\frac{d_X}{d_X + 1}\left(\frac{1}{d_A} + \frac{1}{d_B}\right) \leqslant u + \bar{u} \leqslant 1. \tag{27}$$

This bound is tight and the quantum CUP set $\mathcal{C}$ intersects the bounding lines at $(1, 0)$, $(0, 1)$ and when $d_A = d_B$ it also attains the optimal hiding point $(u, \bar{u}) = (\frac{d_X}{d_A(d_X+1)}, \frac{d_X}{d_A(d_X+1)})$.

The proof of this is provided in Appendix B 1. These bounds place hard limits on the amount of quantum information that can be hidden in the correlations between systems, and also how it can be shared between local systems. The upper bound can be directly related to the no-cloning theorem, as if $u = 1$ for the identity channel then necessarily $\bar{u} = 0$ and the other marginal is completely depolarizing.

The perfect hiding point (0,0) is always precluded from the (isometric) CUP set, which is a consequence of the no-hiding theorem. Further, the upper bound can always be saturated using the bipartite identity and swap channels, while the lower bound can be saturated in the case $d_X = d_A = d_B = d$ via a $d^2$-dimensional generalization of the controlled-NOT operation.

In the case of equal subsystem dimensions, the quantum CUP set is further restricted.

*Theorem IV.2 (No-hiding bound on quantum CUP set $\mathcal{C}$).* Given any input system $X$ and output systems $A$ and $B$ all of equal dimension. The associated quantum CUP set $\mathcal{C}$ is confined such that for

$$(u, \bar{u}) = (0, x) \Rightarrow x = 1. \tag{28}$$

Proof given in Appendix B 1. This restriction on quantum CUP sets encapsulates both the no-hiding theorem in the following manner. The no-hiding theorem here states that if one marginal channel contains no information about the input system, then necessarily all the information can be recovered through the other marginal channel [26]. Therefore when $d_X = d_A = d_B$, if $\mathcal{E} = \mathcal{D}$ then necessarily $\bar{\mathcal{E}} = \mathcal{U}$, a unitary. From Theorem IV.2, a quantum CUP set captures this geometrically, as for the point $(0, x)$ in $\mathcal{C}$ then $x = 1$ only. Which corresponds exactly (and only) to $\mathcal{E} = \mathcal{D}$ and $\bar{\mathcal{E}} = \mathcal{U}$, thereby capturing the no-hiding theorem.

### C. The simplest quantum CUP set

The simplest quantum CUP set, with nontrivial bipartite outputs, is the case $d_X = d_A = d_B = 2$. From Theorem IV.1, for the (isometric) CUP set $\mathcal{C}$, this gives the following bounds:

$$\tfrac{2}{3} \leqslant u + \bar{u} \leqslant 1 \tag{29}$$

with the optimal hiding point given by $(u, \bar{u}) = (1/3, 1/3)$.

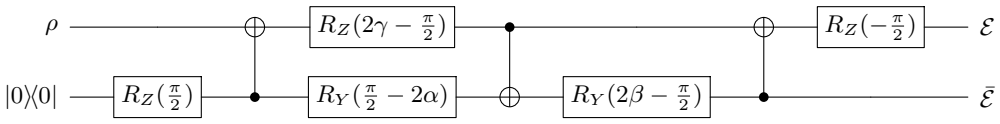


FIG. 2. Circuit decomposition for generic 2 qubit isometry $\mathcal{V}(\alpha, \beta, \gamma)$. For $d_X = d_A = d_B = 2$, all isometries can be expressed in the above form, where $0 \leqslant \alpha, \beta, \gamma \leqslant \pi$ [60]. The complementary channels $\mathcal{E} = \mathrm{tr}_B \circ \mathcal{V}$ and $\bar{\mathcal{E}} = \mathrm{tr}_A \circ \mathcal{V}$ are shown, by ranging over $\alpha, \beta, \gamma$ we can generate the CUP set $\mathcal{C}$ for 1 to 2 qubits.

For isometries mapping single qubit to two qubits, $\mathcal{V}(\rho) := \mathcal{U}_{AB}(\rho \otimes |0\rangle\langle 0|)$, it is sufficient to range over all unitaries $\mathcal{U}_{AB}$ to explore the full parameter space of $(u, \bar{u})$ for $\mathcal{C}$. The general form of two qubit unitaries contains at most three CNOTs and three independently parametrised single qubit rotations [60] (see Fig. 2). However, the two parameter isometry set with $\mathcal{U}_{AB} = \mathcal{U}_{AB}(\alpha, \beta)$ (for $\alpha, \beta \in \mathbb{R}$) (with circuit as in Fig. 3 below) generates all possible complementary channel pairs, up to local unitaries [60]. As the CUP set is invariant under local unitaries, this family suffices to fully describe it. We plot in Fig. 4 the shape of this simplest CUP set, which we obtain by numerically ranging over all $\alpha$ and $\beta$.

In Fig. 4, three boundary curves can be identified. The families of channels generating the boundary are of interest for structural reasons and will be key to the experimental implementation we devise. The curved upper curve is given by a smooth interpolation between the identity channel and the SWAP channel that simply swaps the outputs on $A$ and $B$. More precisely it is given by $\mathcal{U}_{AB} = \mathrm{SWAP}^{\alpha}$ for $0 \leqslant u \leqslant 1$ and $0 \leqslant \alpha \leqslant 1$. The analytical relationship between $u$ and $\bar{u}$ for the upper curve is

$$(u, \bar{u}) = (u, 3 + u - 2\sqrt{1 + 3u}). \tag{30}$$

The analytical relationship between $u$ and $\bar{u}$ for the lower curves is linear, as shown in Fig. 4. The lower-right curve is given by $\mathcal{U}_{AB} = \mathrm{CNOT}^{\alpha}_{AB}$, over the domain $\frac{1}{3} \leqslant u \leqslant 1$. While the left curve is given by $\mathcal{U}_{AB} = \mathrm{CNOT}^{\alpha}_{BA} \circ \mathrm{CNOT}_{AB}$ over the domain $0 \leqslant u \leqslant \frac{1}{3}$. The derivations of the boundary curves are provided in Appendix D.

### D. The reversible CUPset

A general reversible quantum CUP set $\mathcal{C}_r$ (where $d_A$, $d_B$, and $d_X$ are not necessarily equal) is given by considering the marginals of the set of globally reversible channels. For $d_X < d_A d_B$ this set will be strictly larger than the set of isometric channels. The set of reversible quantum channels has been fully characterized [51]: $\mathcal{R}$ is a reversible channel if and only if there is a unitary $U$ and a *mixed* state $\sigma$,

$$\mathcal{R}(\rho) = U(\rho \otimes \sigma)U^{\dagger}. \tag{31}$$

Restricting $\sigma$ to a pure state gives the smaller set of isometric channels. As a consequence, as for classical theory, we can always write any reversible channel $\mathcal{R}$ as the convex combination of isometries $\mathcal{R} = \sum_i^r p_i \mathcal{V}_i$ (see Corollary C.2). Therefore we can think of the reversible CUP set $\mathcal{C}_r$ as introducing auxiliary classical randomness to the isometric CUP set $\mathcal{C}$. We analytically show that any point $(u, \bar{u})$ in $\mathcal{C}_r$ will obey the same upper bound as $\mathcal{C}$ (see Corollary C.2)—adding randomness does not increase our ability to clone information. However, the existence of a nontrivial lower bound for $\mathcal{C}_r$, and therefore the possibility of perfect hiding, will depend on the values of $d_A$, $d_B$, and $d_X$.

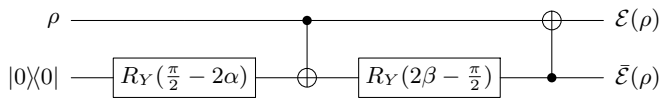


FIG. 3. Sufficient circuit decomposition for 2 qubit isometry $\mathcal{V}(\alpha, \beta)$. For $d_X = d_A = d_B = 2$, the above isometry is sufficient to generate all points of the CUP set $(u, \bar{u})$ with $0 \leqslant \alpha, \beta \leqslant \pi$ [60]. This follows from the general decomposition given in Fig. 2 below, observing that the initial two gates do not change the state of the system, and the invariance of unitarity under local unitaries.

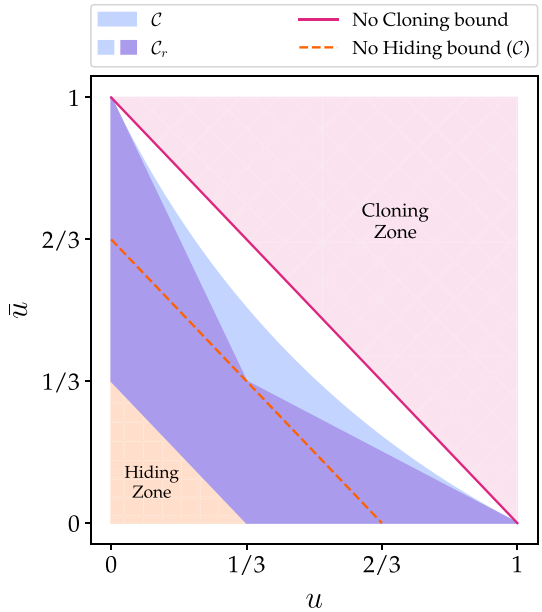


FIG. 4. Quantum CUP sets. The simplest isometric and reversible CUP sets under quantum theory, with their analytical bounds ($d_X = d_A = d_B = 2$). The CUP set $\mathcal{C}$ generated by global isometries is the central boomerang-shaped region (blue). Extending this to reversible operations $\mathcal{C}_r$ increases the set in the direction of (0,0) to the boundary with the Hiding zone (yellow). The two diagonal red lines are obtained from the general analytic upper and lower bounds for CUP sets in quantum theory. In contrast, for classical theory we have that $\mathcal{C}_r$ is the border of the unit square, while $\mathcal{C}$ is the triple of points (1, 1), (1, 0), (0, 1).

#### 1. Perfect hiding with classical randomness

In the case $d_X = d_A = d$ and $d_B = d^2$, the reversible CUP set $\mathcal{C}_r$ contains the point (0,0) and perfect hiding can be achieved. However, as the channel is both nonunitary and not isometric, it does not constitute a violation of the no-hiding theorem. The following channel illustrates the perfect hiding channel when $d = 2$, and can be generalized.

Labeling the four Pauli operators on a single qubit as $\{P_i\} = \{\mathbb{1}, X, Y, Z\}$ we randomly apply an operator to the input state and record which to a classical register, such that

$$\mathcal{R}(\rho) = \frac{1}{4}\sum_i^4 P_i \rho P_i \otimes |i\rangle\langle i|, \tag{32}$$

where $\{|i\rangle\langle i|\}$ are the four computational basis states on two qubits. This channel has maximally mixed marginals, $\mathrm{tr}_A[\mathcal{R}(\rho)] = \mathbb{1}/2$ and $\mathrm{tr}_B[\mathcal{R}(\rho)] = \mathbb{1}/4$. Thus $(u, \bar{u}) = (0, 0)$. However, there exists a quantum channel $\mathcal{R}'$ such that $\mathcal{R}' \circ \mathcal{R}(\rho) = \rho$ for any state $\rho$. Physically, $\mathcal{R}'$ is implemented by measuring the classical register $B$, and applying the corresponding Pauli operator to system $A$, then discarding the register. The Kraus operators, $\mathcal{R}'(\cdot) = \sum_i R'_i \cdot R'^{\dagger}_i$, for this channel will be of the form

$$\{R'_i\} = \{P_i \otimes \langle i|\}. \tag{33}$$

It is readily seen that $\sum_i R'^{\dagger}_i R'_i = 1$.

We can connect any channel, to a isometric CUP set in a higher dimension through the Stinespring dilation. The following isometry

$$V = \frac{1}{4}\sum_i^4 P_i \otimes |i\rangle_B \otimes |i\rangle_C \tag{34}$$

gives $\mathcal{R}(\rho) = \mathrm{tr}_C[V\rho V^{\dagger}]$ where the dimension of subsystem $C$ is $d_C = 4$. However, by tracing out the $A$ subsystem, we find $\rho$ can be completely recovered in $BC$. In fact, any bipartite combination of the subsystems $A$, $B$ and $C$ defines a pair of marginal channels for the isometric CUP sets $\mathcal{C}$ with dimensions (2,16) or (4,8). The lower bound on isometric CUP sets given in Theorem IV.1 then guarantees that there is no arrangement of $A$, $B$ and $C$ such that both marginals are completely depolarising—confirming that quantum information cannot be completely hidden, and can always be recovered fully in the unitary dynamics of the larger system.

#### 2. Boundaries of the simplest reversible CUP set

In the case $d_X = d_A = d_B = 2$, the reversible quantum CUP set $\mathcal{C}_r$ is quite similar to $\mathcal{C}$. It has exactly the same upper boundary but different lower boundaries, which are again straight lines. We have the following analytical bounds for reversible CUPs of these dimensions

$$\tfrac{1}{3} \leqslant u + \bar{u} \leqslant 1. \tag{35}$$

Where the lower bound can be found algebraically from the general circuit decomposition of a unitary on two qubits and using the characterization theorem of reversible channels.

The lower bounding curves are straight lines, and given by considering the marginal unitarities of the reversible channel $\mathcal{R}(\rho) = \mathcal{U}_{AB}(\rho \otimes \frac{\mathbb{1}}{2})$. The right-lower surface is given by $\mathcal{U}_{AB} = \mathrm{CNOT}^{\alpha}_{AB}$ over the domain $\frac{1}{3} \leqslant u \leqslant 1$. The middle-lower surface is $\mathcal{U}_{AB} = \mathrm{CNOT}^{\alpha}_{BA} \circ \mathrm{CNOT}_{AB}$ for $0 \leqslant u \leqslant \frac{1}{3}$. Finally, the left surface is given by $\mathcal{U}_{AB} = \mathrm{CNOT}^{\alpha}_{AB} \circ \mathrm{CNOT}_{BA} \circ \mathrm{CNOT}_{AB}$ for $u = 0$.

A similar construction to the lower boundaries of this reversible CUP set appears in the context of interleaved fidelity randomized benchmarking [61].

### E. The full CUP set

Finally, the full quantum CUP set $\mathcal{C}_*$ is given by the marginal unitarities of any quantum channel from a system $X$ to a joint system $AB$. We have the following analytical bounds, which constrain full CUP sets, with proofs given in Appendix B 3.

*Theorem IV.3 (No-cloning bound on full quantum CUP set $\mathcal{C}_*$).* Given any input system $X$ and output systems $A$ and $B$. The associated full quantum CUP set $\mathcal{C}_*$ is confined such that for

$$(u, \bar{u}) = (1, x) \Rightarrow x = 0. \tag{36}$$

Therefore, similar to $\mathcal{C}$ and $\mathcal{C}_r$, the full CUP set $\mathcal{C}_*$ captures the impossibility of perfect cloning under quantum theory; as if $u = 1$ for one marginal being the identity channel then necessarily $u = 0$ for the other marginal being completely depolarizing.

We conjecture that the full CUP set obeys the same analytical upper bound as the isometric and reversible CUP sets given in Theorem IV.1. However, the proof does not generalize straightforwardly. In the case of equal subsystem dimensions—which is relevant for partial cloning processes—we have the following result that in the limit of large system sizes converges to the conjectured bound.

*Theorem IV.4 (General bound on full quantum CUP set $\mathcal{C}_*$).* Given any input system $X$ and output systems $A$ and $B$ with equal dimensions $d_X = d_A = d_B = d$. The associated full quantum CUP set $\mathcal{C}_* \subseteq [0, 1]^2$ is confined in the $(u, \bar{u})$ plane by

$$u + \bar{u} \leqslant 1 + \frac{1}{d+1}. \tag{37}$$

This bound places a general limit on how quantum information, quantified through the unitarity, can be distributed between two parties using any quantum channel.

It is readily seen that there is no lower hiding bound on a full CUP set by considering a partially depolarizing channel on each output subsystem, as discussed in Sec. V A.

### F. Partial cloning

Throughout this section we have derived bounds on quantum CUP sets, which we have related to quantum incompatibility and how quantum information can be distributed between two parties using different families of quantum channels. As a special case, we can consider partially cloning two copies of an unknown quantum state in the following way.

Asymmetric state independent *partial cloning* [62] of two copies of a quantum state will be given by setting $d_X = d_A = d_B = d$ and requiring that the marginals channels $\mathcal{E}$ and $\bar{\mathcal{E}}$ both be partially depolarizing such that

$$\mathcal{E}(\rho) = p\rho + (1-p)\frac{\mathbb{1}}{d}, \quad \bar{\mathcal{E}}(\rho) = q\rho + (1-q)\frac{\mathbb{1}}{d}, \tag{38}$$

for $0 \leqslant p, q \leqslant 1$ [62–64]. Note that, from the no-cloning theorem, if $p = 1$ then necessarily $q = 0$ and vice versa. The optimality of a partially cloning process is typically assessed through the fidelity of the output states with the target state [65,66]; for state independent cloning this is equivalent to assessing the average gate fidelities, $f(\mathcal{E})$ and $f(\bar{\mathcal{E}})$, or finding the maximal value of $p + q$.

The fidelity of a quantum channel is upper bounded by the unitarity [36] such that

$$\left(\frac{df(\mathcal{E}) - 1}{d - 1}\right)^2 \leqslant u(\mathcal{E}) \equiv u \tag{39}$$

and similarly for $\bar{u}$. Moreover, we have equality for a partially depolarizing channel with $u = p^2$. Therefore any bound on the sum of CUPs immediately gives a bound on the fidelities possible for partial cloning. When we consider any partial cloning process ($\mathcal{C}_*$)—ranging over of all CPTP maps—we have the bound in Theorem IV.4 such that

$$p^2 + q^2 \leqslant 1 + \frac{1}{d+1}. \tag{40}$$

We can compare this bound to results from the literature. The optimal (with respect to fidelity) symmetric partial cloning process can be shown [66–68] to yield $p = q = (d + 2)/2(d + 1)$ giving

$$p^2 + q^2 = \frac{1}{2}\left(1 + \frac{1}{d+1}\right)^2. \tag{41}$$

Therefore the bound in Eq. (40) maintains a separation from the optimal value for $d > 1$. If we restrict to isometric ($\mathcal{C}$) or reversible ($\mathcal{C}_r$) partial cloning processes we have a bound of $p^2 + q^2 \leqslant 1$, which is tight, from Theorem IV.1.

Alternatively, we can consider the optimality of partial cloning with respect to unitarity—such that we maximize $u + \bar{u}$ directly. This may be different to using fidelity as unitarity is a quadratic measure of a channel. For example, the case of partially cloning two copies of a qubit state with a 1 to 2 qubit reversible channel is captured by the simplest CUP sets decomposed in Sec. IV C. We can read off that the optimal reversible partially cloning process with respect to unitarity is the isometry $\mathcal{V}(\rho) = SWAP^{\alpha}(\rho \otimes \sigma)$ up to local unitaries on the outputs and where $\sigma$ is any pure qubit state. From Fig. 4, we observe that $u + \bar{u}$ is maximized only for $\alpha = 0$ or $\alpha = 1$ when no partial cloning occurs. Therefore when using unitarity as a measure of optimality, all partial cloning situations are sub-optimal compared with simply copying the input state to one output system. This suggests that when partially cloning some quantum information must necessarily be "lost" in the correlations between the output states.

## V. DIRECT QUANTUM CUP SET ESTIMATION THROUGH STATE PURITY MEASUREMENTS

Having established the relationship between CUP sets, no-go theorems and quantum incompatibility, we now address the estimation of quantum CUP sets. In this section, we use formulations of unitarity in terms of quantum state purities to directly estimate the individual terms. Our simulations using IBMQ focus on two qubit systems, as this allows for the smallest nontrivial quantum CUP set. In all cases we use the IBMQ model of device noise, derived from the performance of the corresponding real world device—such that there are errors on the gateset, in the preparation of states, and in their measurement. The minimal circuit decompositions generating the boundary of the isometric quantum CUP sets are shown in Figs. 5 and 6.

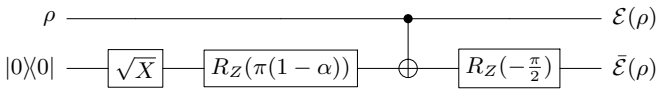


FIG. 5. Circuit decomposition in IBM gateset for lower right CUP set surface. Circuit for 2 qubit isometry $\text{CNOT}^{\alpha}_{AB}(\rho \otimes |0\rangle\langle 0|)$, and complementary channels $\mathcal{E}$ and $\bar{\mathcal{E}}$ for the lower right surface of the CUP set are shown. The final $R_Z$ rotation is optional but aids in the estimation of CUPs through spectral techniques.

### A. Effects of noise

The methods for estimating CUP sets we employ can be separated into two stages: (i) the preparation of the channels that generate the CUP set, (ii) the estimation of the prepared channel's unitarity. There will be errors associated with both (i) and (ii). The errors in (i) are our primary interest as they place a limit on the device's performance at estimating CUPs. However, for the direct methods we cannot easily distinguish between these errors, so refer to a noisy version, $(\cdot)_N$, of the whole process $(u_N, \bar{u}_N)$ for estimating $(u, \bar{u})$.

The simplest way to model how noise affects CUP sets is through a depolarizing channel given by

$$\mathcal{D}_p := (1 - p)id + p\mathcal{D}, \tag{42}$$

where $id(\rho) = \rho$ and $\mathcal{D}(\rho) = \sigma$, for $\sigma$ another fixed quantum state. Given $u(id \circ \mathcal{E}) = u(\mathcal{E} \circ id) = u(\mathcal{E})$ and $u(\mathcal{D} \circ \mathcal{E}) = u(\mathcal{E} \circ \mathcal{D}) = u(\mathcal{D}) = 0$ then for any CUP set we have

$$\begin{aligned}(u_N, \bar{u}_N) &= (u(\mathcal{D}_{p_A} \circ \mathcal{E}), u(\mathcal{D}_{p_B} \circ \bar{\mathcal{E}})), \\ &= ((1 - p_A)^2 u, (1 - p_B)^2 \bar{u}).\end{aligned} \tag{43}$$

Therefore by varying $p_A$ and $p_B$ independently a CUP set can be projected towards either axis or towards the origin, as illustrated in Fig. 7. As this allows us to reach any point in the full CUP set ($\mathcal{C}_*$), we can use depolarization as a crude way to quantify how "noisy" an estimated CUP set is ($\mathcal{C}$ or $\mathcal{C}_r$).

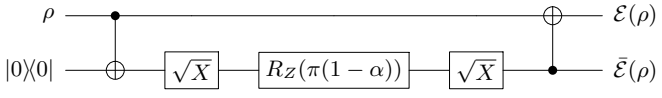


FIG. 6. Circuit decomposition in IBM gateset for lower left CUP set surface. Circuit for 2 qubit isometry $\text{CNOT}^{\alpha}_{BA} \circ \text{CNOT}_{AB}(\rho \otimes |0\rangle\langle 0|)$, and complementary channels $\mathcal{E}$ and $\bar{\mathcal{E}}$ for the lower left surface of the CUP set are shown.

### B. Estimation through complementarity formulation

For any quantum channel $\mathcal{E}$ (with input dimension $d_X$) we can express the unitarity in terms of purities as

$$u(\mathcal{E}) = \frac{d_X}{d_X^2 - 1}\left(d_X \gamma\left(\tilde{\mathcal{E}}\left(\frac{\mathbb{1}}{d_X}\right)\right) - \gamma\left(\mathcal{E}\left(\frac{\mathbb{1}}{d_X}\right)\right)\right), \quad (44)$$

where $\tilde{\mathcal{E}}$ is any channel complementary to $\mathcal{E}$ [50]. For the isometric CUP set, $\mathcal{C}$, any compatible pair of channels $(\mathcal{E}, \bar{\mathcal{E}})$ will be complementary to each other. Therefore, by estimating the two purity terms in Eq. (44) we get the point $(u, \bar{u})$.

The purity of a quantum state can be estimated through a SWAP test [17]. For two unknown quantum states, $\rho$ and $\sigma$, the following circuit performs a SWAP test of the states

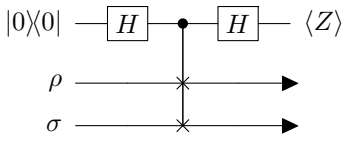


(45)

giving $\langle Z \rangle = \mathrm{tr}[\rho\sigma]$, for the expectation value of Pauli $Z$ measured on the first qubit. The central gate is the controlled *SWAP* (or Fredkin) gate.

With $\rho = \sigma = \mathcal{E}(\mathbb{1}/2)$ or $\rho = \sigma = \bar{\mathcal{E}}(\mathbb{1}/2)$ (restricting to the case $d_X = d_A = d_B = 2$), we can use the SWAP test circuit on a quantum device to get direct, albeit noisy, estimation $(u_N, \bar{u}_N)$ of a point $(u, \bar{u})$ of the CUP set. This, however, requires the preparation of the maximally mixed state, which we discuss in Sec. V D.

### C. Estimation through Choi state formulation

For the reversible CUP set $\mathcal{C}_r$, the resulting compatible pair of channels $(\mathcal{E}, \bar{\mathcal{E}})$ are not necessarily complementary to each other. While it is straightforward to derive complementary channels for the families of channels we consider, the number of purity terms to be estimated from Eq. (44) doubles compared to $\mathcal{C}$. Further, these new complementary channels will necessarily have a larger dimension, thereby increasing the complexity of the SWAP test. However, equivalently, and perhaps more naturally, we can formulate an approach using only the channels $(\mathcal{E}, \bar{\mathcal{E}})$ through the Choi-Jamiołkowski isomorphism.

For any quantum channel $\mathcal{E}$ (with input dimension $d_X$) we have

$$u(\mathcal{E}) = \frac{d_X}{d_X^2 - 1}\left(d_X \gamma(\mathcal{J}(\mathcal{E})) - \gamma\left(\mathcal{E}\left(\frac{\mathbb{1}}{d_X}\right)\right)\right), \quad (46)$$

where $\mathcal{J}(\mathcal{E})$ is the Choi-Jamiołkowski state of the channel $\mathcal{E}$ (given in Appendix C) [50].

Restricting to $d_X = d_A = d_B = 2$, from Eq. (45) we can estimate the first purity by preparing two copies of the Choi state, e.g., $\rho = \sigma = \mathcal{J}(\mathcal{E})$. For a channel with dimension $d$, the Choi state has dimension $d^2$, therefore the number of target qubits in the controlled *SWAP* for $\mathcal{C}_r$ is doubled compared to estimating $\mathcal{C}$. The second term in Eq. (45) can be obtained from $\rho = \sigma = \mathcal{E}(\mathbb{1}/2)$. As this process must be repeated for $u(\bar{\mathcal{E}})$, estimating points on $\mathcal{C}_r$ will generally require twice the number of experiments of $\mathcal{C}$.

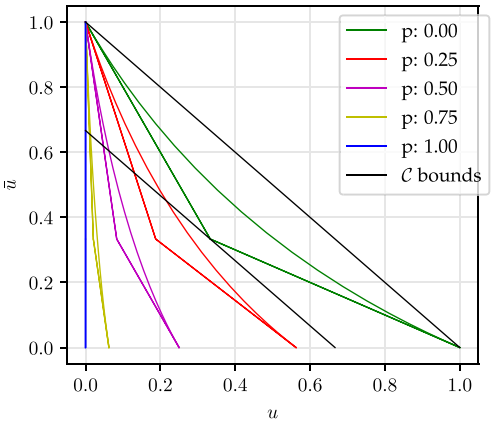


FIG. 7. CUP set deformation through depolarization. The simplest CUP set $\mathcal{C}$ is shown when one output is depolarized, $[u(\mathcal{D}_p \circ \mathcal{E}), u(\bar{\mathcal{E}})]$ for different values of $p$.

### D. Preparation of the maximally mixed state and experimental results

Both of the above methods require the preparation of the maximally mixed state. With a unitary circuit, we can do this (i) statistically, by averaging the results of experiments performed on computational basis states, or (ii) by discarding information about a prepared pure state (e.g., a marginal state of a Bell state). The former method requires more experiments while the later introduces further uncertainty into the estimation.

We use (i) to estimate the isometric CUP set $\mathcal{C}$ using complementarity formulation, as it requires a smaller system size. The exact circuits for the complete purity estimations are given in Fig. 8(a). We then experimentally estimate a range of CUPs on the surface of the CUP set $\mathcal{C}$ on a simulated IBM device. The results of this experiment are shown in Fig. 9(a) where a partially depolarizing model has been fitted to each surface.

Then we pair (ii) with estimation through the Choi state. The exact circuits for this method are given in Fig. 8(b). We again estimate a range of CUPs on the surface of the reversible CUP set $\mathcal{C}_r$. The results of this experiment are shown in Fig, 9(b) where a partially depolarizing model has been fitted to each surface. A comparison of the resources required for each direct method is given in Table I.

### E. Discussion of direct methods

The direct methods we have implemented have a few sources of errors. For any estimated CUP, $(u_N, \bar{u}_N)$, the largest error, in terms of the size of intended operation, will be on the controlled SWAP gate(s). Secondly, as the SWAP test relies upon the final measurement being taken in the correct basis, the direct methods are sensitive to even small final SPAM errors.

Examining Fig. 9 we observe variance in the data, even after a round of averaging over 100 experimental runs has been performed. The lack of robustness to SPAM errors, means that we cannot ascribe this variance to one source—it may come primarily from SPAM $[u_N \approx u_N(\mathcal{E})]$ or it may occur in the preparation of the channel itself $[u_N \approx u(\mathcal{E}_N)]$. This is the main weakness with the direct methods, compared to methods we discuss in the following section.

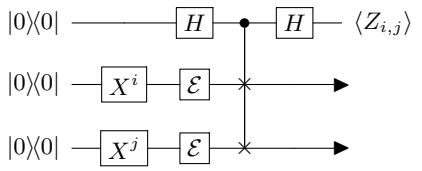


(a) For $X^1 = X$ & $X^0 = id$, four settings of the above circuit give an estimation of $\gamma(\mathcal{E}(\mathbb{1}/2))$ through the relation $\frac{1}{4}(\langle Z_{0,0}\rangle + \langle Z_{0,1}\rangle + \langle Z_{1,0}\rangle + \langle Z_{1,1}\rangle) = \gamma(\mathcal{E}(\mathbb{1}/2))$.

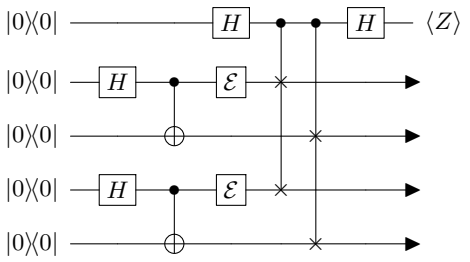


(b) The above circuit gives an estimation of the Choi state purity through $\langle Z\rangle = \gamma(\mathcal{J}(\mathcal{E}))$.

FIG. 8. Circuits for estimation of unitarity $u(\mathcal{E})$ of single qubit channel $\mathcal{E}$ through state purity relations.

However, we note that even after the depolarizing fit is applied, for both $\mathcal{C}$ and $\mathcal{C}_r$ the noisy estimated CUP set is found strictly below the no-cloning upper bound, and therefore in the full CUP set $\mathcal{C}_*$.

The size of parameters needed for the depolarizing fit let us compare between the estimation of $\mathcal{C}$ and $\mathcal{C}_r$. From Table II, the estimated depolarization is two to three times higher for $\mathcal{C}_r$. As the channels required to generate $\mathcal{C}_r$ are very similar to $\mathcal{C}$, we can prescribe this increase directly to the larger overhead and complexity of the protocol for $\mathcal{C}_r$.

Finally, we note that the direct methods rely on a SWAP test(s), and are therefore not efficiently scaleable in number of qubits.

## VI. SPAM ROBUST CUP SET ESTIMATION

With the direct method of the previous section, we make no distinction between errors in the implementation of the target channel, and errors in the estimation protocol including initial state preparation and final measurement (SPAM) errors. This severely limits the usefulness of the direct method as a measure of whether a device obeys the CUP set's informational bounds. For example, in the extreme, we could imagine a device that implements any quantum channel perfectly but has SPAM errors such that it applies a final Hadamard transform on all qubits before measurement. With the direct SWAP test method, this would only generate the point (0,0) on the CUP set diagram. From this we might conclude the device is not acting as a closed quantum system—when in fact, prior to measurement, it was performing perfectly.

With the above in mind, in this section we consider protocols to estimate quantum CUP sets that are robust to SPAM errors. However, will see that the SPAM robust protocols come with a cost of much larger operational overheads, and introduce different sources of potential noise compared to the direct methods.

### A. Estimation through randomized benchmarking

Through randomized benchmarking (RB) [35] we can estimate the unitarity $u(\Lambda_C)$ of the average error channel $\Lambda_C$ induced by a computational gateset $\{\mathcal{U}_C\}$ generating the Clifford group.

If we interleave a target channel of fixed dimension $\mathcal{E}$ between rounds of random Clifford unitaries in the RB protocol, we can estimate the unitarity of the joint channel $u(\mathcal{E} \circ \Lambda_C)$.

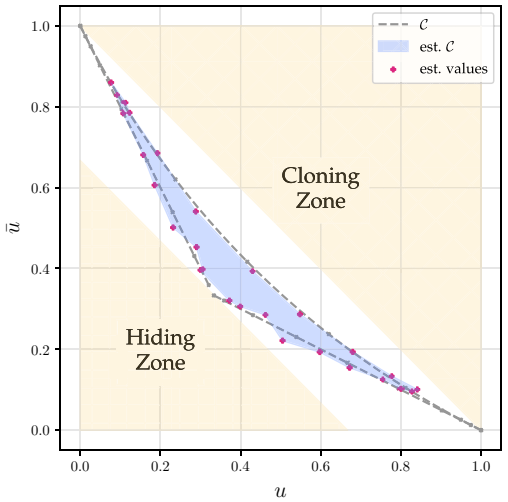


(a) CUP-set ($\mathcal{C}$), estimated with complementary channel method.

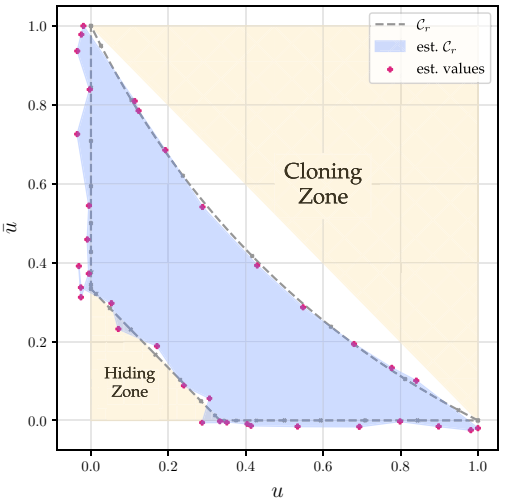


(b) Reversible CUP-set ($\mathcal{C}_r$), estimated with Choi state method.

FIG. 9. Direct estimation of quantum CUP sets. The simplest quantum CUP sets are experimentally estimated directly through SWAP test schemes. A best-fit depolarizing noise model has been applied to each surface (see Table II).

TABLE I. Comparison of total number of experiments undertaken for the estimation of a point on the CUP distribution. For each technique, an experimental scheme was run on a simulation of a quantum device, with device noise imported from IBM Q via qiskit.

| **Technique** | No. of qubits ($\mathcal{C}$) | No. of qubits ($\mathcal{C}_r$) | States | Measurements | Sequences | Repetitions | Shots | **Total Runs** |
|---|---|---|---|---|---|---|---|---|
| Complementarity SWAP | 5 | 7 | 4 | 1 | 1 | 100 | 200 | 80 000 |
| Choi SWAP | 7 | 9 | 1 | 1 | 1 | 100 | 200 | 20 000 |
| Spectral tomography | 2 | 3 | 2 | 3 | 40 | 10 | 200 | 480 000 |
| Interleaved RB | 2 | 3 | 6 | 3 | 10 | 10 | 200 | 360 000 |

Therefore in the limit $\Lambda_C = id$ the interleaved RB protocol returns an exact estimation of $u(\mathcal{E})$. More generally, as unitarity is proportional to the Hilbert-Schmidt norm of the channel's matrix representation we also have the relation $u(\mathcal{E} \circ \Lambda_C) \leqslant u(\mathcal{E})||\Lambda_C||_\infty$, where $||\Lambda_C||_\infty$ corresponds to the largest singular value of the average noisy Clifford gateset channel. This may also be determined, for example via spectral methods as in Sec. VI B to obtain more precise bounds for $u(\mathcal{E})$ in the presence of noisy Clifford operations.

Applying interleaved RB to an estimation of the CUP set follows from the above. However, in addition, it involves an interleaved implementation of $\mathcal{E}$ using an ancilla initialization, the global unitary $\mathcal{U}_{AB}$ and a partial trace. We require the additional assumption that we can perform mid-circuit resets, $\mathcal{D}(\rho) := |0\rangle\langle 0|$, and that the noisy version of these resets are incoherent—in that none of the state $\rho$ is carried through even if $\mathcal{D}$ induces some larger error on the device. This allows us to include the error $\mathcal{D}$ in $\Lambda_C$.

Through interleaved RB we can estimate the unitarity of the following channel in a SPAM robust manner

$$\mathcal{E}_N(\rho) = tr_B \circ \Lambda_{AB} \circ \mathcal{U}_{AB} \circ \Lambda_C(\rho \otimes |0\rangle\langle 0|), \tag{47}$$

where $\Lambda_{AB}$ is the noise channel associated with the experimental implementation of $(\mathcal{E}, \bar{\mathcal{E}})$, the channels generating the (isometric) CUP set. Therefore, in the noiseless limit $\Lambda_C = \Lambda_{AB} = id$ the following protocol returns exactly $u(\mathcal{E})$ in the isometric CUP set $\mathcal{C}$.

Protocol 1: Interleaved unitarity RB for channel $\mathcal{E}(\rho) := \mathrm{tr}_B \circ \mathcal{U}_{AB}(\rho \otimes |0\rangle\langle 0|)$.

1. **Prepare** the system in the state $\rho_A \otimes |0\rangle\langle 0|_B$.
2. **Select** a sequence of length $k$ of random elements of the Clifford group, $\{\mathcal{U}_{C,i}\}$, on subsystem $A$, starting with $k = 1$, while performing a reset on subsystem $B$ after every gate. Such that for each gate $\mathcal{U}_{C,i} \otimes \mathcal{D}$.
3. **Interleave** the bipartite unitary $\mathcal{U}_{AB}$ after every Clifford gate (such that the final gate is a Clifford gate).
4. **Estimate** the square $(m_A)^2$, of the expectation value of an observable $M_A$ on subsystem $A$ for this particular sequence of gates.
5. **Repeat 1, 2, 3, and 4** for many random sequences of the same length, finding the average estimation $\mathbb{E}_\rho[(m_A)^2]$ of $(m_A)^2$.
6. **Repeat 1, 2, 3, 4, and 5** increasing the length of the sequence $k$ by 1.
7. **Fit** the data $\mathbb{E}_\rho[(m_A)^2] = c_0 + c_1 s^{k-1}$ where $c_0, c_1$ are real constants, and find the estimated unitarity $s$.

The above protocol gives the decay parameter that estimates $s = u(\mathcal{E}_N)$ for the noisy channel $\mathcal{E}_N$, which includes the device errors from preparation of the channel $\mathcal{E}$, but also protocol-specific errors coming from the noisy random Cliffords.

The protocol for $\bar{\mathcal{E}}$ is very similar (see Appendix E) but requires an additional *SWAP* operation after each interleaved unitary, and the resource costs associated with it. Allowing us to estimate $u(\bar{\mathcal{E}}_N)$ for

$$\bar{\mathcal{E}}_N(\rho) = tr_A \circ \Lambda_{AB} \circ \mathcal{U}_{AB} \circ \Lambda_C(\rho \otimes |0\rangle\langle 0|). \tag{48}$$

Proofs showing that the above protocols indeed produce estimates of CUP sets can be found in Appendix E. An examination of how the protocols behave under gate independent noise is given in Appendix E 3.

We implement these protocols on a simulated version of the IBM Belem device, in an efficient manner (see Appendix E 2) [36]. The results of the experiment for $\mathcal{C}$ are shown in Fig. 10(a), and for $\mathcal{C}_r$ in Fig. 10(b), where a depolarization model has been fitted to each surface. A comparison of the resources used for each experiment can be found in Table I.

### B. Estimation through spectral methods

We next discuss if spectral methods (that estimate eigenvalues of a channel) are an alternative SPAM robust path to estimate CUP sets. We include several results that link unitarity to quantities estimable through spectral tomography [46], which may be of independent interest.

#### 1. Unitarity and channel eigenvalues

Any quantum channel $\mathcal{E}$: $\mathcal{B}(\mathcal{H}) \to \mathcal{B}(\mathcal{H})$ on a system $\mathcal{H}$ of dimension $d$ has a (Liouville) representation as a $d^2 \times d^2$ matrix. Its nonunital $d^2 - 1 \times d^2 - 1$ block $T_\mathcal{E}$ has eigenvalues $\{\lambda_i(\mathcal{E})\}$ that are real or come in complex conjugate pairs [69]. The following bound (with proof given in Appendix C) holds for all quantum channels of fixed dimension.

*Lemma VI.1.* For any quantum channel $\mathcal{E}$, of fixed dimension $d$ and any unitary channels $\mathcal{U}$ and $\mathcal{V}$ we have

$$u(\mathcal{E}) \geqslant \sum_{k=1}^{d^2-1} \frac{|\lambda_k(\mathcal{U} \circ \mathcal{E} \circ \mathcal{V})|^2}{d^2 - 1}. \tag{49}$$

Further, for a single qubit channel $\mathcal{E}$, we can improve upon this bound:

*Theorem VI.1 (Variational formulation).* For any single qubit quantum channel $\mathcal{E}$, maximizing over all single qubit unitary channels $\{\mathcal{U}_i\}$ gives

$$u(\mathcal{E}) = \max_{\mathcal{U}_i, \mathcal{U}_j} \sum_{k=1}^{3} \frac{|\lambda_k(\mathcal{U}_i \circ \mathcal{E} \circ \mathcal{U}_j)|^2}{3}. \tag{50}$$

TABLE II. Depolarization fits for noisy CUP sets. For each experimental estimation of the quantum CUP sets $\mathcal{C}$ and $\mathcal{C}_r$ we fit a depolarizing noise model $(u_N, \bar{u}_N) = ((1-p_A)^2 u, (1-p_B)^2 \bar{u})$ to each surface (see Sec. V A). Best fit values for $(p_A, p_B)$ are tabulated here.

| | Upper | $\mathcal{C}$ Left | $\mathcal{C}$ Right | $\mathcal{C}_r$ Left | $\mathcal{C}_r$ Middle | $\mathcal{C}_r$ Right |
|---|---|---|---|---|---|---|
| Interleaved RB | (0.063,0.137) | (0.032,0.125) | (0.095,0.159) | (0,0.015) | (0.047,0.107) | (0,0) |
| SWAP test | (0.165,0.147) | (0.073,0.160) | (0.084,0.153) | (0,0.562) | (0.365,0.337) | (0.253,0) |

Proof given in Appendix C. The practical application of Theorem VI.1 to the channels that generate the CUP set is shown in Fig. 11.

#### 2. *Estimation of CUP set through spectral tomography*

Putting this together, a spectral protocol to estimate the CUP set would require the following steps. For any point, estimate the eigenvalues of the channel $\mathcal{U}_i \circ \mathcal{E} \circ \mathcal{U}_j$ through spectral tomography for $N$ different randomly chosen $\mathcal{U}_i$ and $\mathcal{U}_j$. From Lemma VI.1, the set of estimated eigenvalues provide a lower bound on $u(\mathcal{E}_N)$ where $\mathcal{E}_N$ is a noisy experimental implementation of $\mathcal{U}_i \circ \mathcal{E} \circ \mathcal{U}_j$. Repeat for $\bar{\mathcal{E}}$ to obtain a lower bound on $u(\bar{\mathcal{E}}_N)$ similarly. For $N \to \infty$, and in practice for at most $N \approx 100$ (see Fig. 11), from Theorem VI.1 the estimated lower bound becomes an estimation of exactly the required unitarities.

We performed the above sequence of spectral tomographic experiments on a simulated version of the IBMQ device, IBM Belem. However, using a similar number of resources to the interleaved RB protocol, we were unable to extract eigenvalues accurately from the tomographic data. We suspect this was due to the finite sampling of expectation values, as for state vector simulations (without sampling) we were able to extract eigenvalues correctly. While increasing the number of shots may therefore help, the experimental overhead would be greatly increased compared to the other SPAM robust techniques we consider.

### C. Discussion of SPAM robust methods

We now briefly discuss the limitations of the interleaved randomized benchmarking technique we give for estimating CUP sets. While the protocol is robust to SPAM errors, it relies on mid-circuit measurements to perform resets, which must be incoherent (but can be noisy). Under this assumption, the decay parameter of the protocol gives a robust estimation of the unitarity of the given channel, $s = u(\mathcal{E}_N)$. If, as we might expect on a NISQ device, the reset allows some coherent information through, then the decay parameter can no longer be directly related to the unitarity, e.g., $s = u_N(\mathcal{E}_N)$. For further discussion see Appendix E 3.

For the channels $(\mathcal{E}_N, \bar{\mathcal{E}}_N)$ to be close (in terms of unitarity) to the channels that generate the CUP set $(\mathcal{E}, \bar{\mathcal{E}})$, we need the error $\Lambda_C$ on one qubit Clifford unitaries to be small. As the error preparing $(\mathcal{E}, \bar{\mathcal{E}})$ should be of similar size to $\Lambda_C$, then we expect that the approximately half of the depolarizing fit required in Fig. 10 can be attributed to the preparation of $(\mathcal{E}, \bar{\mathcal{E}})$.

### D. Comparison with direct methods

While the SPAM robust methods require an additional assumption about the nature of resets on the device, this is a vast improvement over the direct methods of Sec. V, where errors arising in the protocol and in the channel preparation could not be separated. The estimation of each CUP set obtained through interleaved RB is also significantly better in terms

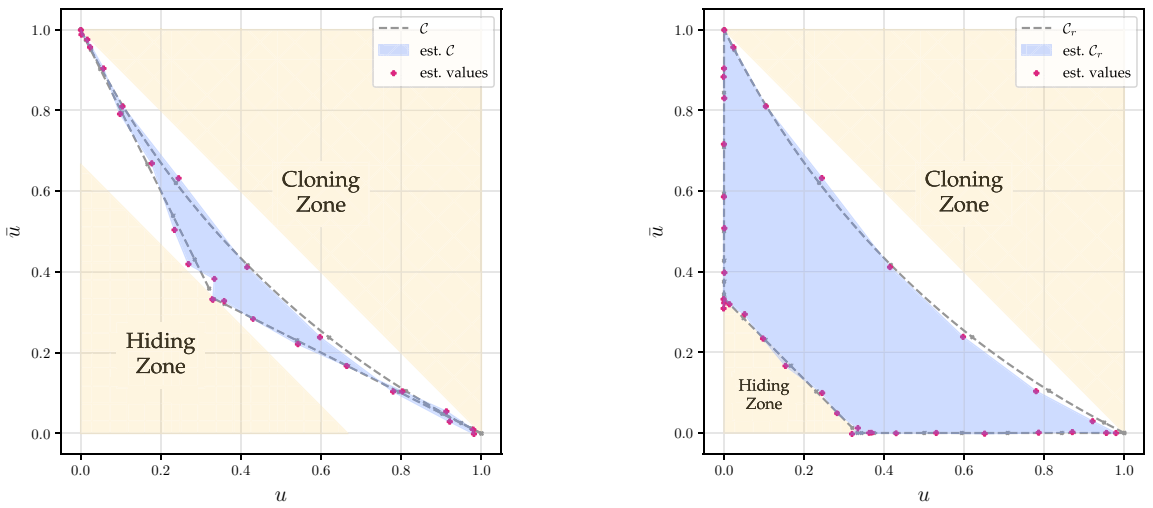


(a) CUP-set ($\mathcal{C}$) (b) Reversible CUP-set ($\mathcal{C}_r$)

FIG. 10. SPAM robust estimation of quantum CUP sets. The simplest quantum CUP sets are experimentally estimated through an interleaved unitarity randomized benchmarking scheme. A best-fit depolarizing noise model has been fitted to each surface (see Table II), where each surface is produced from 9 pairs of experimental values.

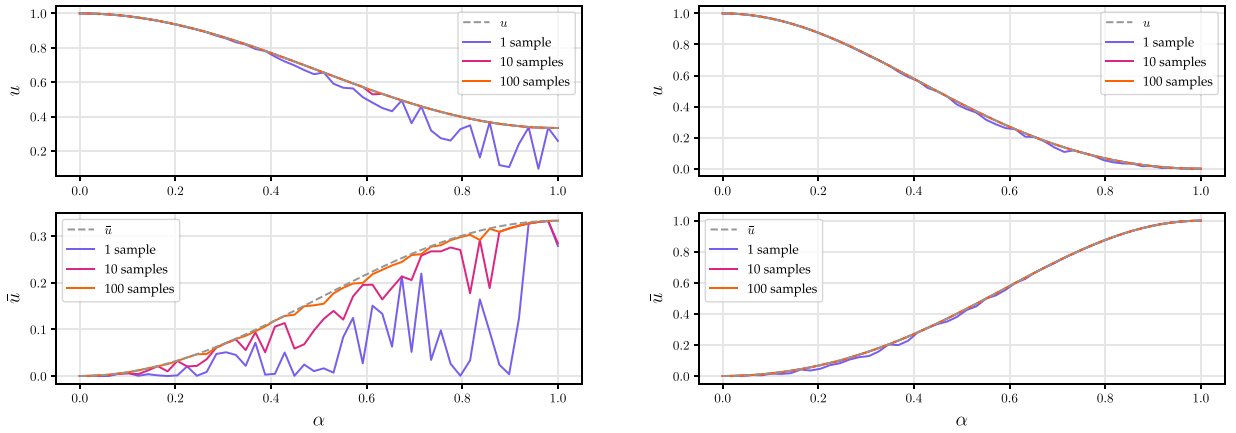


(a) $\mathcal{U}_{AB} = CNOT^{\alpha}_{AB}$ (b) $\mathcal{U}_{AB} = SWAP^{\alpha}$

FIG. 11. Bound on CUP set through random unitaries. For two surfaces of the CUP set $\mathcal{C}$ (for a range of 50 discrete values of $0 \leqslant \alpha \leqslant 1$) we can test how quickly the lower bound given in Lemma VI.1 converges towards the actual unitarity given in Theorem VI.1. Roughly, we observe, for bound within 1% of the unitarity we need one random setting if $u > 2/3$, and at most 100 random settings for lower values.

of the required depolarizing fit than the direct methods (see Table II). The variance in the data points is also significantly lower for interleaved RB, even when performing an additional round of averaging for the direct methods.

Additionally, we see that the interleaved RB protocol is very good at estimating points where $u$ or $\bar{u} = 0$, especially compared to the direct methods. This is likely due to the fact that, for the direct methods, these points require the estimation of two nonzero purities for any value of $u$, whereas the SPAM robust methods estimate a single decay parameter.

## VII. OUTLOOK

### A. The long arm of purity

One way of viewing the approach we have taken here, is that we are starting with the concept of purity and applying it with greater and greater abstraction in the sequence

$$\text{States} \rightarrow \text{Channels} \rightarrow \text{Theories}. \tag{51}$$

Let us make this more precise. In any general theory we can begin with an elementary notion of disorder of a state, which can be quantified via the purity $\gamma(x)$. This can now be extended to the channel level for the theory and we obtain the unitarity $u(\mathcal{E})$, which is the natural generalization of purity. Indeed if we view a state $x$ as itself being a preparation *channel* $1 \rightarrow x$ from the trivial system to $S$ then it is readily seen that we have that $u(x) = \gamma(x)$ and the two notions coincide. For more nontrivial channels it can be shown [50] that the unitarity coincides with the conditional purity of the Choi state of $\mathcal{E}$. The unitarity is a variance-based measure of the disorder of a channel from one input system to one output system.

We next extend this further to consider how order can be shared or distributed amongst subsystems $A$ and $B$ of a theory and unitarity pairs $(u, \bar{u})$, and subsets of channels. Again, this is a generalization of the preceding concept since if $B$ is the trivial system then $(u, \bar{u}) = (u(\mathcal{E}), 0)$, which is just the unitarity of a channel. When applied to *sets* of channels this leads to encodings of no-go results of the theory. In this sense CUP sets are purity measures of a given physical theory within the space of all operational theories.

### B. Conclusions

We have derived a simple formulation of information disturbance and incompatibility in quantum theory, given through the set of *compatible unitarity pairs* (CUPs). These pairs of compatible channels can be defined in any generalized probability theory, and they capture key limits of information transformation under the chosen theory.

We undertook a thorough comparison between CUP sets under quantum theory, where they are tightly bound, and classical theory where the CUP set lies on the boundary of the unit square. We then explored the CUP set for quantum theory in detail, including general bounds on these sets, which we related to quantum no-go theorems.

As the CUP set encapsulates fundamental incompatibility limits of quantum theory, it may be used as a tool for benchmarking quantum devices. To this aim, we showed how the quantum CUP set can be estimated through simple and direct purity methods, but also in a SPAM robust way through interleaved randomized benchmarking of unitarity. While estimating many points on the CUP set may not be an efficient method of benchmarking, the extremal points [given for the qubit case by (0,1), (1,0), and $(1/3, 1/3)$], requires just six experiments. The extremal points capture both the core CUP set geometry and the unitarity-based information disturbance relation given in Theorem IV.1, and therefore are a natural minimal set. Future work will focus on implementing the estimation methods for CUP set on different quantum hardware. In particular, we may also consider randomized measurements [70] for direct purity estimation, which would give an additional method to produce the CUP set, with minimal implementation overhead.

Recently, many theoretical results have analyzed how the effect of noise on quantum algorithms results in a computation that can be efficiently simulated classically [71]. This behavior remains even for quantum advantage experiments [72].

Similarly, we have seen that noise affects the quantum CUP set by shifting it towards regions that exhibit classical behavior such as hiding. An interesting future direction would be to connect these two aspects and determine if device benchmarking via CUP sets can provide additional information to bound finite size classical simulability of quantum circuits in the presence of noise.

While we expect classical devices to perform a perfect estimation of the isometric CUP set, the reversible classical CUP set relies on a source of randomness to perform perfect hiding. The accuracy of the estimated CUP set can then be directly related to the bias in the randomness. Therefore the CUP set formulation may also be useful as a diagnostic tool in assessing the quality of a source of randomness.

Finally, in this paper we primarily considered two theories, classical theory and quantum theory; however, CUP sets can be derived for more general physical theories. It would be interesting to see how the structure of CUP sets varies between different theories.

## ACKNOWLEDGMENTS

We thank Roger Colbeck for useful discussions on perfect hiding in quantum theory. M.G. is funded by a Royal Society Studentship. D.J. was supported by the Royal Society and also a University Academic Fellowship. We acknowledge the use of IBM Quantum services for this work. We thank Matty Hoban, Daniel Mills, and anonymous reviewers for useful feedback on this manuscript.

## APPENDIX A: GENERAL INCOMPATIBILITY AND REVERSIBILITY

### 1. A general definition of unitarity

Generalized probability theories (GPTs) provide a broad framework in which one can compare different physical theories and study their fundamental properties from an abstract, often information-theoretic viewpoint [39]. Our primary aim is to capture incompatibility, and no-go theorems through measures, which, at least for quantum theory, can be efficiently computed and are robust to noise. However, our paper can be framed in a general GPT setting, which we explore in this section.

A GPT is defined by a closed, convex set $\mathcal{S}$ of states, and an effects space $E$, from which the allowed measurements on $\mathcal{S}$ are constructed. The extremal points of $\mathcal{S}$ are called the pure states, and we denote this set by $\partial\mathcal{S}$. We shall further assume that we can embed both the state space $\mathcal{S}$ and effects space $E$ in a Euclidean vector space, with inner product $\langle\cdot,\cdot\rangle$. A measurement $\mathcal{M}$ is given by any tuple of effects $\mathcal{M} = \{m_1, m_2, ..., m_N\}$ with $m_i \in E$ such that $\sum_k^N \langle m_k, x\rangle = 1$ for all states $x$ in $\mathcal{S}$. The probability of getting an outcome $m_k$ on a state $x$ is given by $p(m_k|x) = \langle m_k, x\rangle$. The dimension $d$ of the state space is given by be the maximal number of completely distinguishable states $\{x_1, x_2, ..., x_d\}$ in $\mathcal{S}$, where a set of states is completely distinguishable if there is a measurement $\mathcal{M}^\sharp = \{m_1, m_2, ..., m_d\}$ that unambiguously identifies which of the states was measured through its deterministic outcome. We call $\mathcal{M}^\sharp$ a *sharp* measurement. Any physical process corresponds to a channel $\mathcal{E}$, which is a linear map that sends any valid state $x$ in the input system to another valid state $\mathcal{E}(x)$ in the output system.

We define the following function, the *purity* $\gamma(x)$ of a state $x$ via

$$\gamma(x) := \max_{\mathcal{M}^\sharp} \sum_k \langle m_k, x\rangle^2, \tag{A1}$$

where the maximization is taken over all sharp measurements $\mathcal{M}^\sharp = \{m_k\}$ in the theory [73]. While this optimization is nontrivial it turns out that the optimal measurements are simply the measurement of the pure states in classical theory, and the rank-1 projective measurement in the eigenbasis of the state in the case of quantum theory (see Lemma A.4). Additionally we can define a generalized maximally mixed state for any GPT obtained by averaging over the pure states $\partial\mathcal{S}$ of the theory

$$\eta := \int_{\partial\mathcal{S}} d\mu(x)\, x. \tag{A2}$$

Together Eqs. (A1) and (A2) allow for the unitarity of a channel to be calculated for theories, which do not have an inner product purity $\langle x, x\rangle$. More generally, the constant $\alpha$ in the definition of unitarity given in Eq. (4) will generally depend on the structure of the state space $\mathcal{S}$ and the measure $d\mu(x)$.

The way in which the state space of subsystems relates to the state space of the global system is slightly nontrivial, and the details can be found in [39,40,74–76]. For composite systems we also have the notion of tracing out or discarding of subsystems, that corresponds to the unit effect. Sometimes for clarity, we put subscripts to specify the systems involved, so that $x_A$ is a state for system $A$ and $x_{ABC}$ is a state for a tripartite system $ABC$. For a state $x_{AB}$ on a bipartite system $AB$ we assume there is channel $x_{AB} \to \mathrm{tr}_A[x_{AB}] =: x_B$ that outputs a state $x_B$ on $B$ that results from discarding or ignoring system $A$. This amounts to computing the marginal of a probability distribution. We also define the identity channel as $id(x) = x$ for all $x \in \mathcal{S}$. Given a channel $\mathcal{E}$ from a subsystem $X$ to subsystems $AB$ we define the *marginal channels* as

$$\mathcal{E}_A(x) := \mathrm{tr}_B \circ \mathcal{E}(x), \tag{A3}$$

$$\mathcal{E}_B(x) := \mathrm{tr}_A \circ \mathcal{E}(x). \tag{A4}$$

### 2. Channel compatibility in general theories

While recent papers deal with incompatibility of measurements in general theories [7,8], one can also extend to the notion of (in)compatible channels [77]. Two (or more) channels in a theory are *compatible* if they arise as marginal channels of a valid global channel within the theory.

Given the structure of the perfect-hiding channel in classical theory, we therefore argue that to capture no-go theorems, the appropriate set of global channels to consider in a theory is the set of reversible channels. In any theory, we say a channel $\mathcal{E}$ is *reversible* precisely if there is a second channel $\mathcal{F}$ in the theory such that $\mathcal{F} \circ \mathcal{E}(x) = x$ for all states $x \in \mathcal{S}$. A particular subset of reversible channels are *isometry* channels $\mathcal{V}$, which preserve the inner product structure, i.e., for any pair of states $y, z$ it satisfies $\langle y, z\rangle = \langle \mathcal{V}(y), \mathcal{V}(z)\rangle$.

We also note that perfect cloning in classical theory involves an isometry channel, while perfect hiding in classical

theory involves a nonisometric, but reversible channel. Therefore if we restricted to isometric channels in a theory this would suggest that is impossible to hide a bit in classical theory, which is not true.

In light of this, we say that a theory admits perfect cloning precisely if there is a channel $\mathcal{E}$ from a system $X$ into a bipartite system $AB$ such that the marginal channels are both the identity channel. We also say that the theory admits perfect hiding precisely if there is a reversible channel $\mathcal{R}$ from $X$ into $AB$ with marginals being two completely erasing channels $\mathcal{D}_1$ from $X$ into $A$ and $\mathcal{D}_2$ from $X$ into $B$. Here a channel $\mathcal{D}$ is completely erasing if for all $x \in \mathcal{S}$ we have $\mathcal{D}(x) = y$ for some fixed $y$.

For quantum theory, a channel $\mathcal{E}$ is reversible if and only if

$$\langle \mathcal{E}(\rho), \mathcal{E}(\tau)\rangle = c\langle \rho, \tau\rangle \tag{A5}$$

for all states $\rho, \tau$ and some constant $c > 0$ [51]. Here the inner product is the Hilbert-Schmidt inner product given by $\langle X, Y\rangle := \mathrm{tr}[X^\dagger Y]$. The latter demonstrates that reversible channels are a natural generalization of isometry channels, for which $c = 1$.

### 3. Properties of unitarity for GPT channels

*Lemma A.1.* For any GPT in which $d\mu(x)$ is nonzero over all of $\partial S$ we have that $u(\mathcal{E}) = 0$ if and only if $\mathcal{E} = \mathcal{D}$ a completely depolarizing channel $\mathcal{D}(y) = z$ for all states $y$, and $z$ fixed.

*Proof.* A sum of non-negative numbers is zero if and only if each number is identically zero. Therefore we have that $u(\mathcal{E}) = 0$ if and only if $\langle m_k, \mathcal{E}(x-\eta)\rangle = 0$ for all $m_k$ in the optimal measurement and for all $x \in \partial S$. Since $m_k \neq 0$ for all $k$ this means that $u(\mathcal{E}) = 0$ if and only if $\mathcal{E}(x-\eta) = 0$ for all $x$, which is true if and only if $\mathcal{E}(x) = \mathcal{E}(\eta) = y$ for all $x$ and fixed $y$. ∎

*Lemma A.2.* For any GPT in which $d\mu(x)$ is nonzero over all of $\partial S$ we have $u(p\mathcal{E} + (1-p)\mathcal{D}) = p^2 u(\mathcal{E})$, where $\mathcal{E}$ is any channel, and $\mathcal{D}$ is a completely depolarizing channel $\mathcal{D}(y) = z$ for all states $y$ with $z$ fixed.

*Proof.* The proof follows from the expansion of the definition of unitarity under linearity, and that $\mathcal{D}(x-\eta) = 0$ (from Lemma A.1). Putting this together

$$\begin{aligned} &u(p\mathcal{E} + (1-p)\mathcal{D}) \\ &:= \alpha \int_{\partial\mathcal{S}} d\mu(x)\, \gamma(p\mathcal{E}(x-\eta) + (1-p)\mathcal{D}(x-\eta)), \\ &= \alpha \int_{\partial\mathcal{S}} d\mu(x)\, \max_{\mathcal{M}^\sharp} \sum_k \langle m_k, p\mathcal{E}(x-\eta)\rangle^2, \\ &= p^2\alpha \int_{\partial\mathcal{S}} d\mu(x)\, \max_{\mathcal{M}^\sharp} \sum_k \langle m_k, \mathcal{E}(x-\eta)\rangle^2 = p^2 u(\mathcal{E}). \end{aligned} \tag{A6}$$

∎

*Corollary A.1.* For any CUP set if the global channel $\mathcal{E}$ from $X \to AB$ gives the point $(u, \bar{u})$ then the set of convex mixtures $p\mathcal{E} + (1-p)\mathcal{D}$ gives the point $(p^2\, u, p^2\, \bar{u})$, where $\mathcal{D}$ is a global completely depolarizing channel $\mathcal{D}(y) = z$ for all states $y$ with $z$ fixed.

*Proof.* This follows from Lemma A.2 with the observation that the marginals $\mathrm{tr}_A \circ \mathcal{D}$ and $\mathrm{tr}_B \circ \mathcal{D}$ of a completely depolarizing channel are also completely depolarizing channels (to a different fixed state). ∎

*Lemma A.3.* Consider a GPT in which $\gamma(x) = \langle x, x\rangle$. Then for any isometry, $\mathcal{V}$, and any other channel, $\mathcal{E}$, we have $u(\mathcal{V} \circ \mathcal{E}) = u(\mathcal{E})$.

*Proof.* The proof also follows from expansion of the definition of unitarity under linearity, and that $\langle \mathcal{V}(x), \mathcal{V}(x)\rangle = \langle x, x\rangle$ for all isometries $\mathcal{V}$ and states $x$. Then

$$\begin{aligned} u(\mathcal{V}\circ\mathcal{E}) &= \alpha \int_{\partial\mathcal{S}} d\mu(x)\, \gamma(\mathcal{V}(x-\eta)), \\ &= \alpha \int_{\partial\mathcal{S}} d\mu(x)\, \langle \mathcal{V}\circ\mathcal{E}(x-\eta), \mathcal{V}\circ\mathcal{E}(x-\eta)\rangle, \\ &= \alpha \int_{\partial\mathcal{S}} d\mu(x)\, \langle \mathcal{E}(x-\eta), \mathcal{E}(x-\eta)\rangle, \\ &= \alpha \int_{\partial\mathcal{S}} d\mu(x)\, \gamma(\mathcal{E}(x-\eta)) = u(\mathcal{E}). \end{aligned} \tag{A7}$$

∎

*Corollary A.2.* Consider a GPT in which $\gamma(x) = \langle x, x\rangle$. Then for any isometry, $\mathcal{V}$, we have $u(\mathcal{V}) = 1$.

*Proof.* This follows from Lemma A.3 with $\mathcal{E} = id$, noting that $u(id) = \alpha \int_{\partial\mathcal{S}} d\mu(x)\, \gamma(x-\eta)$. ∎

### 4. Sharp measurements for quantum theory

*Lemma A.4.* For any quantum state $\rho$ of dimension $d$ we have

$$\max_{\mathcal{M}^\sharp} \sum_k \langle m_k, \rho\rangle^2 = \mathrm{tr}[\rho]^2, \tag{A8}$$

where the maximization is taken over all sharp measurements $\mathcal{M}^\sharp = \{m_k\}$ of dimension $d$.

*Proof.* We can write any quantum state in its eigenbasis, $\rho = \sum_i^d \lambda_i |e_i\rangle\langle e_i|$, such that $\mathrm{tr}[\rho]^2 = \sum_i^d \lambda_i^2$. As $\mathcal{M}^\sharp$ completely distinguishes $d$ states we have

$$\begin{aligned} \max_{\mathcal{M}^\sharp} \sum_k \langle m_k, \rho\rangle^2 &= \max_{\mathcal{M}^\sharp} \sum_k^d (\sum_i^d \lambda_i \mathrm{tr}[m_k^\dagger |e_i\rangle\langle e_i|])^2, \\ &= \max_M \sum_k^d (\sum_i^d \lambda_i M_{ki})^2, \end{aligned} \tag{A9}$$

where $M_{ki} := \mathrm{tr}[m_k^\dagger |e_i\rangle\langle e_i|]$, and forms a doubly stochastic matrix where $\sum_i^d M_{ki} = \sum_k^d M_{ki} = 1$. Expanding the purity

$$\begin{aligned} \max_{\mathcal{M}^\sharp} \sum_k \langle m_k, \rho\rangle^2 &= \max_M \sum_{i,j,k}^d \lambda_i\lambda_j M_{ki} M_{kj}, \\ &= \max_M \sum_{i,j}^d \lambda_i\lambda_j (M^T M)_{ij}. \end{aligned} \tag{A10}$$

As the product of any two doubly stochastic matrices is doubly stochastic, $\sum_i (M^T M)_{ij} = \sum_j (M^T M)_{ij} = 1$. We then use that the vector $\lambda = (\lambda_1, \lambda_2, ..., \lambda_d)^T$ majorizes the vector

$\mu := M^T M\lambda$. Such that

$$\max_{\mathcal{M}^\sharp} \sum_k \langle m_k, \rho\rangle^2 = \sum_i \lambda_i\mu_i \leqslant \sum_i \frac{\lambda_i^2+\mu_i^2}{2} \leqslant \sum_i \lambda_i^2. \tag{A11}$$

Where the last inequality follows the Schur-convexity of $f(x) = x^2$. Equality holds as we can choose the measurement in the eigenbasis, which attains the bound. ■

## APPENDIX B: PROPERTIES OF QUANTUM CUP SETS

### 1. Information disturbance and no-go bounds on isometric CUP set

*Theorem B.1 (General incompatibility bound on isometric quantum CUP set $\mathcal{C}$).* Given any input system $X$ of dimension $d_X$ and output systems $A$ and $B$ of dimensions $d_A, d_B$, with $d_X \leqslant d_A d_B$. The associated quantum CUP set $\mathcal{Q} \subseteq [0,1]^2$ is confined to the band in the $(u, \bar{u})$ plane defined by

$$\frac{d_X}{d_X+1}\left(\frac{1}{d_A}+\frac{1}{d_B}\right) \leqslant u+\bar{u} \leqslant 1. \tag{B1}$$

This bound is tight and the CUP set $\mathcal{Q}$ intersects the bounding lines at $(1,0), (0,1)$ and when $d_A = d_B$ it also attains the optimal hiding point $(\frac{d_X}{d_A(d_X+1)}, \frac{d_X}{d_A(d_X+1)})$.

*Proof.* It can be shown [50] that the unitarity of a channel can be expressed as

$$u(\mathcal{E}) = \frac{d_X}{d_X^2-1}(d_X \mathrm{tr}[\tilde{\mathcal{E}}(\mathbb{1}/d_X)^2] - \mathrm{tr}[\mathcal{E}(\mathbb{1}/d_X)^2]) \tag{B2}$$

where $\tilde{\mathcal{E}}$ is any complementary channel to $\mathcal{E}$, which we can choose to be $\bar{\mathcal{E}}$. Applying the above expression to the complementary pair $(\mathcal{E}, \bar{\mathcal{E}})$ we then have that

$$u(\mathcal{E})+u(\bar{\mathcal{E}}) = \frac{d_X}{d_X+1}(\mathrm{tr}[\mathcal{E}(\mathbb{1}/d_X)^2] + \mathrm{tr}[\bar{\mathcal{E}}(\mathbb{1}/d_X)^2]). \tag{B3}$$

For the lower bound, we bound each purity term individually. For any quantum state $\rho$ for a system of dimension $d$ we have the purity is lower bounded as $\mathrm{tr}[\rho^2] \geqslant 1/d$, and therefore

$$u(\mathcal{E})+u(\bar{\mathcal{E}}) \geqslant \frac{d_X}{d_X+1}\left(\frac{1}{d_A}+\frac{1}{d_B}\right). \tag{B4}$$

For the upper bound, we use the following property of complementary channels. We have that $\mathcal{E} := \mathrm{tr}_B \circ \mathcal{V}_{X\to AB}$ and $\bar{\mathcal{E}} := \mathrm{tr}_A \circ \mathcal{V}_{X\to AB}$ for an isometric channel $\mathcal{V}_{X\to AB}$. Therefore the state $\rho_{AB} = \mathcal{V}_{X\to AB}(\mathbb{1}/d_X)$ has the marginals $\rho_A = \mathcal{E}(\mathbb{1}/d_X)$ and $\rho_B = \bar{\mathcal{E}}(\mathbb{1}/d_X)$. For a general bipartite quantum state $\rho_{AB}$ we have [78] that

$$\gamma(\rho_A)+\gamma(\rho_B) \leqslant 1+\gamma(\rho_{AB}), \tag{B5}$$

and therefore

$$u(\mathcal{E})+u(\bar{\mathcal{E}}) \leqslant \frac{d_X}{d_X+1}(1+\gamma(\mathcal{V}_{X\to AB}(\mathbb{1}/d_X))). \tag{B6}$$

As $\mathcal{V}_{X\to AB}$ is an isometry

$$\gamma(\mathcal{V}_{X\to AB}(\mathbb{1}/d_X)) = \mathrm{tr}[(V(\mathbb{1}/d_X)V^\dagger)^2] = \frac{1}{d_X}. \tag{B7}$$

Substituting this into the previous inequality we obtain

$$u(\mathcal{E})+u(\bar{\mathcal{E}}) \leqslant 1, \tag{B8}$$

which completes the proof. ■

*Lemma B.1.* Any isometry $\mathcal{V}_{X\to AB}$ from an input system $X$ and joint output system $AB$ with equal dimensions $d_X = d_A = d_B = d$, defines the complementary fixed dimension channels $\mathcal{E} := tr_B \circ \mathcal{V}_{X\to AB}$ and $\bar{\mathcal{E}} := tr_A \circ \mathcal{V}_{X\to AB}$. The pair $\mathcal{E}$ and $\bar{\mathcal{E}}$ obey the following equivalence relations:

$$\begin{array}{ccc} \mathcal{E}=\mathcal{U} & \Longleftrightarrow & \bar{\mathcal{E}}=\mathcal{D} \\ \Updownarrow & & \Updownarrow \\ u(\mathcal{E})=1 & \Longleftrightarrow & u(\bar{\mathcal{E}})=0 \end{array} \tag{B9}$$

where $\mathcal{D}(\rho) = \sigma$ is a completely depolarizing channel to a fixed state $\sigma$.

*Proof.* We first prove $\mathcal{E} = \mathcal{U} \iff \bar{\mathcal{E}} = \mathcal{D}_\psi$. Note that for any quantum channel $\mathcal{F}$, its complementary channel $\tilde{\mathcal{F}}$ is unique up to an isometry on the output of $\tilde{\mathcal{F}}$ [79]. Further, we can write any isometry from $n = \log d$ to $2n$ qubits in the form $\mathcal{V}_{X\to AB}(\rho) = \mathcal{U}_{AB}(\rho \otimes |0\rangle\langle 0|^{\otimes n})$. Therefore it suffices to find any fixed dimension channel $\tilde{\mathcal{E}}$ complementary to $\mathcal{E}$, and apply a final unitary rotation. The isometry $\mathcal{V}_{X\to AB} = \mathcal{U}_A \otimes \mathcal{U}_B(\rho \otimes |0\rangle\langle 0|^{\otimes n}) = \mathcal{U}_A(\rho) \otimes \mathcal{U}_B(|0\rangle\langle 0|^{\otimes n})$ where $\mathcal{U}_A$ and $\mathcal{U}_B$ are unitaries on the respective subsystems $A$ and $B$, gives the required form for $\mathcal{E}$, and we are free to set $\mathcal{U}_B(|0\rangle\langle 0|) = |\psi\rangle\langle\psi|$, which is the exact form of $\bar{\mathcal{E}}$. Applying the same argument starting from $\bar{\mathcal{E}}$ completes the inverse direction.

We now prove $\mathcal{E} = \mathcal{U} \iff u(\mathcal{E}) = 1$. For any quantum channel we have $\mathcal{F} = \mathcal{V} \iff u(\mathcal{F}) = 1$ for any isometry $\mathcal{V}$ [50]. For fixed input and output dimensions the set of isometric channels is equivalent to the set of unitary channels, which completes the proof.

Finally, we prove $\bar{\mathcal{E}} = \mathcal{D}_\psi \iff u(\bar{\mathcal{E}}) = 0$. For any quantum channel we have $\mathcal{F} = \mathcal{D} \iff u(\mathcal{F}) = 0$ for any completely depolarizing channel $\mathcal{D}(\rho) := \sigma$ to a fixed (potentially mixed) state $\sigma$. However, given the form of $\mathcal{V}_{X\to AB}$ the only marginal channel that can be constructed that disregards any input state completely is given by $\bar{\mathcal{E}}(\rho) = \mathcal{U}_B(|0\rangle\langle 0|) = |\psi\rangle\langle\psi|$. Therefore all completely depolarizing channels generated by $\mathcal{V}_{X\to AB}$ must be to pure states, $\mathcal{D}_\psi$, and the condition holds.

*Corollary B.1.* Given any input system $X$, and output systems $A$ and $B$ of equal dimension $d_X = d_A = d_B$. The associated (isometric) quantum CUP set $\mathcal{C}$ is confined such that if

$$(u,\bar{u}) = (0,x) \Rightarrow x = 1. \tag{B10}$$

*Proof.* This follows directly from the previous lemma, and the definitions of $u$ and $\bar{u}$. ■

### 2. No-cloning bound on reversible CUP set

*Lemma B.2.* For any convex combination of channels $\mathcal{E} = \sum_i^r p_i\mathcal{E}_i$, the respective $T_\mathcal{E}$ matrix has the form

$$T_\mathcal{E} = \sum_i^r p_i T_{\mathcal{E}_i}. \tag{B11}$$

*Proof.* $T_{\mathcal{E}} = \sum_{j,k}^{d_X^2-1,d_Y^2-1} \langle y_k|\mathcal{E}(x_j)\rangle|y_k\rangle\langle x_j| = \sum_{j,k}^{d_X^2-1,d_Y^2-1} \langle y_k|\sum_i^r p_i\mathcal{E}_i(x_j)\rangle|y_k\rangle\langle x_j|$. However, as quantum channels are linear, this is $\sum_i^r p_i \sum_{j,k}^{d_X^2-1,d_Y^2-1} \langle y_k|\mathcal{E}_i(x_j)\rangle|y_k\rangle\langle x_j| = \sum_i^r p_i T_{\mathcal{E}_i}$. ∎

*Lemma B.3.* The unitarity $u(\mathcal{E})$ is a convex function of any quantum channel $\mathcal{E}$.

*Proof.* From Lemma C.2, for any convex combination of channels $\mathcal{E} = \sum_i^r p_i\mathcal{E}_i$ the corresponding $T_{\mathcal{E}}$ matrix is the convex combination of each individual term, $T_{\mathcal{E}} = \sum_i^r p_i T_{\mathcal{E}_i}$. All norms are convex non-negative functions, including the $l_2$ norm, $||\cdot||$ [80]. Further, if $f(x)$ is convex and non-negative function of $x$ then $f(x)^2$ is also convex. Therefore $||T_{\mathcal{E}}||^2$ is a convex function of $T_{\mathcal{E}}$. Putting this together with the appropriate dimension factor we have

$$u(\mathcal{E}) = \alpha||\sum_i^r p_i T_{\mathcal{E}_i}||^2 \leqslant \sum_i^r p_i\alpha||T_{\mathcal{E}_i}||^2 = \sum_i^r p_i u(\mathcal{E}_i), \tag{B12}$$

which completes the proof.

*Corollary B.2.* Given any input system $X$ and output systems $A$ and $B$, the associated reversible quantum CUP set $\mathcal{C}_r \subseteq [0,1]^2$ is confined in the $(u,\bar{u})$ plane by

$$u + \bar{u} \leqslant 1. \tag{B13}$$

*Proof.* We can always write a reversible channel $\mathcal{R}$ as the convex combination of isometries $\mathcal{V}_i$ as

$$\mathcal{R}(\rho) = \mathcal{U}_{AB}(\rho\otimes\sigma) = \mathcal{U}_{AB}(\rho\otimes\sum_i^r p_i\psi_i)$$
$$= \sum_i^r p_i\mathcal{U}_{AB}(\rho\otimes\psi_i) = \sum_i^r p_i\mathcal{V}_i \tag{B14}$$

for some pure states $\psi_i = |\psi_i\rangle\langle\psi_i|$. Therefore we can write the marginal channel $\mathcal{E}_{\mathcal{R}} := \mathrm{tr}_B\circ\mathcal{R}$ as

$$\mathcal{E}_{\mathcal{R}} = \mathrm{tr}_B\circ\mathcal{R} = \sum_i^r p_i\mathrm{tr}_B\circ\mathcal{V}_i = \sum_i^r p_i\mathcal{E}_i \tag{B15}$$

and similarly for $\bar{\mathcal{E}}_{\mathcal{R}} := \mathrm{tr}_A\circ\mathcal{R}$. As the unitarity is convex

$$u(\mathcal{E}_{\mathcal{R}}) = u(\sum_i^r p_i\mathcal{E}_i) \leqslant \sum_i^r p_i u(\mathcal{E}_i) \tag{B16}$$

and similarly for $\bar{\mathcal{E}}_{\mathcal{R}}$. As $u(\mathcal{E}_i) + u(\bar{\mathcal{E}}_i) \leqslant 1$ for all $i$, we have

$$u(\mathcal{E}_{\mathcal{R}}) + u(\bar{\mathcal{E}}_{\mathcal{R}}) \leqslant \sum_i^r p_i(u(\mathcal{E}_i) + u(\bar{\mathcal{E}}_i)) \leqslant \sum_i^r p_i = 1. \tag{B17}$$

This completes the proof.

### 3. Cloning bounds on full CUP set

*Theorem B.2 (No-cloning bound on full quantum CUP set $\mathcal{C}_*$).* Given any input system $X$ and output systems $A$ and $B$. The associated full quantum CUP set $\mathcal{C}_*$ is confined such that for

$$(u,\bar{u}) = (1,x) \Rightarrow x = 0. \tag{B18}$$

*Proof.* Consider any isometry, $\mathcal{V}$, from system $X$ to a tripartite system $ABC$. Due to the Stinespring dilation, we can set $\mathcal{E} = \mathrm{tr}_{BC}\circ\mathcal{V}$ and $\bar{\mathcal{E}} = \mathrm{tr}_{AC}\circ\mathcal{V}$ to be the channels that generate any full CUP set with $(u,\bar{u}) \equiv (u(\mathcal{E}), u(\bar{\mathcal{E}}))$. We have that $u = u(\mathcal{E}) = 1$ if and only if $\mathcal{E} = \mathcal{U}$ for some isometry, $\mathcal{U}$. The channel $\mathrm{tr}_A\circ\mathcal{V}$ is complementary to $\mathcal{E}$ and from Theorem IV.1 (and as a consequence of [5]) must therefore be completely depolarizing, $\mathrm{tr}_A\circ\mathcal{V} = \mathcal{D}$, to some fixed state. Therefore $\bar{\mathcal{E}} = \mathrm{tr}_{AC}\circ\mathcal{V} = \mathrm{tr}_C\circ\mathcal{D}$. However, the marginal, $\bar{\mathcal{E}} = \mathrm{tr}_C\circ\mathcal{D}$, of any completely depolarizing channel is also a completely depolarizing channel $\bar{\mathcal{E}} = \mathcal{D}'$ to a different fixed state. This ensures $u(\bar{\mathcal{E}}) = 0$, which completes the proof.

*Theorem B.3 (Partial cloning bound on full quantum CUP set $\mathcal{C}_*$).* Given any input system $X$ and output systems $A$ and $B$ with equal dimensions $d_X = d_A = d_B = d$. The associated full quantum CUP set $\mathcal{C}_* \subseteq [0,1]^2$ is confined in the $(u,\bar{u})$ plane by

$$u + \bar{u} \leqslant 1 + \frac{1}{d+1}. \tag{B19}$$

*Proof.* Consider an isometry, $\mathcal{V}$ from system $X$ to a tripartite system $ABC$ where $d_X = d_A = d_B = d$ and the dimension of system $C$ is $d_C$. Due to the Stinespring dilation, we can set $\mathcal{E}_A = \mathrm{tr}_{BC}\circ\mathcal{V}$ and $\mathcal{E}_B = \mathrm{tr}_{AC}\circ\mathcal{V}$ to be the channels that generate the full CUP set with $(u,\bar{u}) \equiv (u(\mathcal{E}_A), u(\mathcal{E}_B))$ in a similar manner to the previous proof. For compactness, we write any marginal channel as $\mathcal{E}_i = \mathrm{tr}_{\neq i}\circ\mathcal{V}$, such as $\mathcal{E}_{BC} = \mathrm{tr}_A\circ\mathcal{V}$. Further, we will write the purity of a marginal channel $\mathcal{E}_i$ acting on the maximally mixed state to be $\gamma_i := \gamma(\mathcal{E}_i(\frac{\mathbb{1}}{d})) = \mathrm{tr}[\mathcal{E}_i(\frac{\mathbb{1}}{d})^2]$. The unitarity $u(\mathcal{E}_i)$ of any marginal channel $\mathcal{E}_i$ is then simply [50]

$$u(\mathcal{E}_i) = \frac{d}{d^2-1}(d\gamma_{\neq i} - \gamma_i). \tag{B20}$$

The unitarities for the full CUP set are then

$$u + \bar{u} = u(\mathcal{E}_A) + u(\mathcal{E}_B) = \frac{d}{d^2-1}(d(\gamma_{BC} + \gamma_{AC}) - \gamma_A - \gamma_B). \tag{B21}$$

We can use a result from the study of the entropy of marginal quantum states to bound this quantity. From Theorem 2 in [81] for any tripartite quantum state $\rho_{ABC}$ with marginal states defined in the usual way, the marginal purities must obey

$$d_A\gamma(\rho_{AC}) + d_B\gamma(\rho_{BC}) \leqslant d_A d_B\gamma(\rho_{ABC}) + \gamma(\rho_C). \tag{B22}$$

Therefore for $\rho_{ABC} = \mathcal{V}(\frac{\mathbb{1}}{d})$ and with subsystems $A$ and $B$ of the same dimension, $d$, we have $d(\gamma_{AC} + \gamma_{BC}) \leqslant d^2\gamma_{ABC} + \gamma_C$. Applying this to Eq. (B21) gives

$$u + \bar{u} \leqslant \frac{d}{d^2-1}(d^2\gamma_{ABC} + \gamma_C - \gamma_A - \gamma_B). \tag{B23}$$

Further, we must have $\gamma_{ABC} = \gamma(\mathcal{V}_{ABC}(\frac{\mathbb{1}}{d})) = \gamma(\frac{\mathbb{1}}{d}) = \frac{1}{d}$ as isometries preserve the inner product. We also have the general bounds of $\frac{1}{d} \leqslant \gamma \leqslant 1$ for any purity of any quantum state of dimension $d$. This gives

$$u + \bar{u} \leqslant \frac{d}{d^2-1}(d + \gamma_C - \gamma_A - \gamma_B),$$
$$\leqslant \frac{d}{d^2-1}\left(d + 1 - \frac{1}{d} - \frac{1}{d}\right) = \frac{d+2}{d+1}. \tag{B24}$$

This completes the proof.

## APPENDIX C: PROPERTIES OF UNITARITY

### 1. Properties of the eigenvalues of $T$ and a bound on unitarity

*Lemma C.1.* For any quantum channel $\mathcal{E}$, of fixed dimension $d$ and unitary channels $\mathcal{U}$ and $\mathcal{V}$ of the same dimension, we have

$$u(\mathcal{E}) \geqslant \sum_{k}^{d^2-1} \frac{|\lambda_k(\mathcal{U}\circ\mathcal{E}\circ\mathcal{V})^2|}{d^2-1}, \tag{C1}$$

where for any quantum channel $\mathcal{F}$, $\{\lambda_k(\mathcal{F})\}$ are the eigenvalues of the associated matrix $T_{\mathcal{F}}$.

*Proof.* For a complex $n\times n$ matrix $A$ with eigenvalues $\{\lambda_k\}$ arranged such that $|\lambda_1| \geqslant ... \geqslant |\lambda_n|$ and singular values $\{\sigma_k\}$ arranged such that $\sigma_1 \geqslant ... \geqslant \sigma_n$. From Weyl's Majorant theorem [82], we have the following majorization:

$$\sum_{i}^{n} |\lambda_i|^p \leqslant \sum_{i}^{n} |\sigma_i|^p \tag{C2}$$

for any $p \geqslant 0$. For any quantum channel $\mathcal{F}$, the unital block $T_{\mathcal{F}}$ is real matrix [83], therefore $\sum_k^{d^2-1} |\lambda_k(\mathcal{F})^2| \leqslant \sum_k^{d^2-1} \sigma_k(\mathcal{F})^2$, where $\lambda_k(\mathcal{F})$ denote eigenvalues and $\sigma_k(\mathcal{F})$ singular values of $T_{\mathcal{F}}$. With $\mathcal{F} = \mathcal{U}\circ\mathcal{E}\circ\mathcal{V}$ for unitary channels $\mathcal{U}$ and $\mathcal{V}$ it follows that

$$\sum_{k}^{d^2-1} |\lambda_k(\mathcal{U}\circ\mathcal{E}\circ\mathcal{V})^2| \leqslant \sum_{k}^{d^2-1} \sigma_k(\mathcal{U}\circ\mathcal{E}\circ\mathcal{V})^2. \tag{C3}$$

However, the singular values are invariant under unitary rotations, therefore

$$\sum_{k}^{d^2-1} \sigma_k(\mathcal{U}\circ\mathcal{E}\circ\mathcal{V})^2 = \sum_{k}^{d^2-1} \sigma_k(\mathcal{E})^2 = (d^2-1)\, u(\mathcal{E}), \tag{C4}$$

which completes the proof. ∎

*Lemma C.2.* For any single qubit quantum channel $\mathcal{E}$, over all single qubit unitary channels $\{\mathcal{U}_i\}$ we have

$$u(\mathcal{E}) = \max_{\mathcal{U}_i,\mathcal{U}_j} \sum_{k}^{3} \frac{|\lambda_k(\mathcal{U}_i\circ\mathcal{E}\circ\mathcal{U}_j)^2|}{3}. \tag{C5}$$

where for any quantum channel $\mathcal{F}$, $\{\lambda_k(\mathcal{F})\}$ are the eigenvalues of the associated matrix $T_{\mathcal{F}}$.

*Proof.* From the previous lemma we have $\sum_k^3 |\lambda_k(\mathcal{U}_i\circ\mathcal{E}\circ\mathcal{U}_j)^2| \leqslant \sum_k^3 \sigma_k(\mathcal{U}_i\circ\mathcal{E}\circ\mathcal{U}_j)^2$ for any $\mathcal{U}_i$ and $\mathcal{U}_j$. However, for any single qubit channel $\mathcal{E}$, we can always find [84] two specific unitaries $\mathcal{U}_1$ and $\mathcal{U}_2$ such that $T_{\mathcal{U}_1\circ\mathcal{E}\circ\mathcal{U}_2}$ is a diagonal matrix, and therefore for which the eigenvalues and singular values coincide $\{\lambda_i(\mathcal{U}_1\circ\mathcal{E}\circ\mathcal{U}_2)\} = \{\sigma_i(\mathcal{U}_1\circ\mathcal{E}\circ\mathcal{U}_2)\}$. This guarantees we can saturate the inequality with

$$\sum_{k}^{3} |\lambda_k(\mathcal{U}_1\circ\mathcal{E}\circ\mathcal{U}_2)^2| = \sum_{k}^{3} \sigma_k(\mathcal{U}_1\circ\mathcal{E}\circ\mathcal{U}_2)^2. \tag{C6}$$

Therefore over two copies the complete set of single qubit unitary channels $\{\mathcal{U}_i\}$, from the above two equations

$$\begin{aligned}\max_{\mathcal{U}_i,\mathcal{U}_j} \sum_{k}^{3} |\lambda_k(\mathcal{U}_i\circ\mathcal{E}\circ\mathcal{U}_j)^2| &= \sum_{k}^{3} \sigma_k(\mathcal{U}_1\circ\mathcal{E}\circ\mathcal{U}_2)^2 \\ &= \sum_{k}^{d^2-1} \sigma_k(\mathcal{E})^2 = (d^2-1)\, u(\mathcal{E}),\end{aligned} \tag{C7}$$

which completes the proof. ∎

### 2. Choi-Jamiołkowski isomorphism

For a quantum channel $\mathcal{E}$ with input dimension $d_X$ the Choi-Jamiołkowski state is given by

$$\mathcal{J}(\mathcal{E}) := \mathcal{E}\otimes id(\psi), \tag{C8}$$

where $\psi = |\psi\rangle\langle\psi|$ with $|\psi\rangle := \frac{1}{\sqrt{d_X}} \sum_i^{d_X} |i\rangle\otimes|i\rangle$, a generalized Bell state [17].

## APPENDIX D: ANALYTICAL FORM OF MARGINAL UNITARITIES FOR SURFACES

### 1. Analytical form for marginal unitarities of SWAP$^\alpha$ isometry

*Lemma D.1.* For the isometry $\mathcal{V}_\alpha(\rho) := \mathrm{SWAP}^\alpha(\rho\otimes|0\rangle\langle 0|)$ where $0 \leqslant \alpha \leqslant 1$, we define the marginals $\mathcal{E}_\alpha(\rho) := \mathrm{tr}_B[\mathcal{V}(\rho)_\alpha]$ and $\bar{\mathcal{E}}_\alpha(\rho) := \mathrm{tr}_A[\mathcal{V}(\rho)_\alpha]$. The unitarities of each marginal are

$$u(\mathcal{E}_\alpha) = \frac{(1-s)(3-s)}{3} \tag{D1}$$

and

$$u(\bar{\mathcal{E}}_\alpha) = 1 - \frac{(1-s)(3+s)}{3} \tag{D2}$$

respectively, where $s = \sin^2(\frac{\pi\alpha}{2})$.

If we consider the sum of the marginals from Lemma E.1 we have

$$u(\mathcal{E}_\alpha) + u(\bar{\mathcal{E}}_\alpha) = 1 - \frac{2s(1-s)}{3} \tag{D3}$$

with $0 \leqslant s \leqslant 1$ and produce a tighter bound on the marginals, namely for any isometry with $d_X = d_A = d_B = 2$, for a given $u(\mathcal{E})$ we have

$$u(\bar{\mathcal{E}}) \leqslant 3 + u(\mathcal{E}) - 2\sqrt{1+3u(\mathcal{E})}. \tag{D4}$$

*Proof.* (of Lemma E.1) First we must obtain a useful analytical form for SWAP$^\alpha$. As SWAP is a unitary channel to derive the analytical form it is sufficient to find the unitary matrix $U$ that transforms the two qubit pure state $|\psi\rangle\otimes|\phi\rangle$ such that

$$U\,|\psi\rangle\otimes|\phi\rangle = |\phi\rangle\otimes|\psi\rangle\,. \tag{D5}$$

From this definition we can write

$$\begin{aligned}U &= |00\rangle\langle 00| + |10\rangle\langle 01| + |01\rangle\langle 10| + |11\rangle\langle 11|, \\ &= \tfrac{1}{2}(\mathbb{1}^{\otimes 2} + X^{\otimes 2} + Y^{\otimes 2} + Z^{\otimes 2}),\end{aligned} \tag{D6}$$

where $\{\mathbb{1}, X, Y, Z\}$ are the Pauli matrices on 1 qubit. Defining the Bell states as $|\Phi_\pm\rangle := \frac{1}{\sqrt{2}}(|00\rangle \pm |11\rangle)$ and $|\Psi_\pm\rangle := \frac{1}{\sqrt{2}}(|01\rangle \pm |10\rangle)$, we can diagonalise this unitary as

$$\begin{aligned} U &= |\Phi_+\rangle\langle\Phi_+| + |\Phi_-\rangle\langle\Phi_-| + |\Psi_+\rangle\langle\Psi_+| - |\Psi_-\rangle\langle\Psi_-|, \\ &= |\Phi_+\rangle\langle\Phi_+| + |\Phi_-\rangle\langle\Phi_-| + |\Psi_+\rangle\langle\Psi_+| + e^{i\pi}|\Psi_-\rangle\langle\Psi_-|. \end{aligned} \tag{D7}$$

As $\text{SWAP}^\alpha(\rho) = U^\alpha \rho (U^\alpha)^\dagger$, up to a global phase we can find [85]

$$U^\alpha = |\Phi_+\rangle\langle\Phi_+| + |\Phi_-\rangle\langle\Phi_-| + |\Psi_+\rangle\langle\Psi_+| + e^{i\pi\alpha}|\Psi_-\rangle\langle\Psi_-|, \tag{D8}$$

and through careful expansion

$$\begin{aligned} U^\alpha &= |00\rangle\langle 00| + |11\rangle\langle 11| + \tfrac{1}{2}(1+e^{i\pi\alpha})(|01\rangle\langle 01| + |10\rangle\langle 10|) + \tfrac{1}{2}(1-e^{i\pi\alpha})(|01\rangle\langle 10| + |10\rangle\langle 01|), \\ &= \tfrac{1}{2}(\mathbb{1}^{\otimes 2} + Z^{\otimes 2}) + \tfrac{1}{4}(1+e^{i\pi\alpha})(\mathbb{1}^{\otimes 2} - Z^{\otimes 2}) + \tfrac{1}{4}(1-e^{i\pi\alpha})(X^{\otimes 2} + Y^{\otimes 2}), \\ &= \tfrac{1}{2}(1+e^{i\pi\alpha})\mathbb{1}^{\otimes 2} + \tfrac{1}{4}(1-e^{i\pi\alpha})(\mathbb{1}^{\otimes 2} + X^{\otimes 2} + Y^{\otimes 2} + Z^{\otimes 2}), \\ &= \tfrac{1}{2}(1+e^{i\pi\alpha})\mathbb{1}^{\otimes 2} + \tfrac{1}{2}(1-e^{i\pi\alpha})U. \end{aligned} \tag{D9}$$

If we now expand the isometry definition we have

$$\begin{aligned} \mathcal{V}(\rho)_\alpha &= U^\alpha \rho \otimes |0\rangle\langle 0| (U^\alpha)^\dagger, \\ &= \left(\frac{1}{2}(1+e^{i\pi\alpha})\right)\mathbb{1}^{\otimes 2} + \frac{1}{2}(1-e^{i\pi\alpha})U)(\rho \otimes |0\rangle\langle 0|)\left(\frac{1}{2}(1+e^{-i\pi\alpha})\mathbb{1}^{\otimes 2} + \frac{1}{2}(1-e^{-i\pi\alpha})U^\dagger\right), \\ &= \cos\left(\frac{\pi\alpha}{2}\right)^2 \mathbb{1}^{\otimes 2}(\rho \otimes |0\rangle\langle 0|)\mathbb{1}^{\otimes 2} + \sin\left(\frac{\pi\alpha}{2}\right)^2 U(\rho \otimes |0\rangle\langle 0|)U^\dagger \\ &\quad + \frac{i}{2}\sin(\pi\alpha)\mathbb{1}^{\otimes 2}(\rho \otimes |0\rangle\langle 0|)U^\dagger - \frac{i}{2}\sin(\pi\alpha)U(\rho \otimes |0\rangle\langle 0|)\mathbb{1}^{\otimes 2}, \\ &= \cos\left(\frac{\pi\alpha}{2}\right)^2 \rho \otimes |0\rangle\langle 0| + \sin\left(\frac{\pi\alpha}{2}\right)^2 |0\rangle\langle 0| \otimes \rho + \frac{i}{2}\sin(\pi\alpha)\mathbb{1}^{\otimes 2}(\rho \otimes |0\rangle\langle 0|)U^\dagger - \frac{i}{2}\sin(\pi\alpha)U(\rho \otimes |0\rangle\langle 0|)\mathbb{1}^{\otimes 2}. \end{aligned} \tag{D10}$$

From this point it is relatively straightforward to show that the unital block $T$ for the 1 qubit channels $\mathcal{E}_\alpha$ and $\bar{\mathcal{E}}_\alpha$ will be

$$T_{\mathcal{E},\alpha} = \begin{array}{c} \\ \langle X/\sqrt{2}| \\ \langle Y/\sqrt{2}| \\ \langle Z/\sqrt{2}| \end{array} \begin{array}{c} \begin{array}{ccc} |X/\sqrt{2}\rangle & |Y/\sqrt{2}\rangle & |Z/\sqrt{2}\rangle \end{array} \\ \begin{pmatrix} \cos\left(\frac{\pi\alpha}{2}\right)^2 & \frac{1}{2}\sin(\pi\alpha) & 0 \\ -\frac{1}{2}\sin(\pi\alpha) & \cos\left(\frac{\pi\alpha}{2}\right)^2 & 0 \\ 0 & 0 & \cos\left(\frac{\pi\alpha}{2}\right)^2 \end{pmatrix} \end{array}, \tag{D11}$$

and

$$T_{\bar{\mathcal{E}},\alpha} = \begin{array}{c} \\ \langle X/\sqrt{2}| \\ \langle Y/\sqrt{2}| \\ \langle Z/\sqrt{2}| \end{array} \begin{array}{c} \begin{array}{ccc} |X/\sqrt{2}\rangle & |Y/\sqrt{2}\rangle & |Z/\sqrt{2}\rangle \end{array} \\ \begin{pmatrix} \sin(\frac{\pi\alpha}{2})^2 & -\frac{1}{2}\sin(\pi\alpha) & 0 \\ \frac{1}{2}\sin(\pi\alpha) & \sin(\frac{\pi\alpha}{2})^2 & 0 \\ 0 & 0 & \sin(\frac{\pi\alpha}{2})^2 \end{pmatrix} \end{array}, \tag{D12}$$

respectively. Therefore the unitarity of $\mathcal{E}_\alpha$ is given by

$$\begin{aligned} u(\mathcal{E}_\alpha) &= \frac{1}{3}\text{tr}[T^\dagger_{\mathcal{E},\alpha} T_{\mathcal{E},\alpha}] \\ &= \cos\left(\frac{\pi\alpha}{2}\right)^4 + \frac{1}{6}\sin(\pi\alpha)^2 \\ &= \frac{1}{6}\cos\left(\frac{\pi\alpha}{2}\right)^2 (5 + \cos(\pi\alpha)). \end{aligned} \tag{D13}$$

For the other marginal, the unitarity of $\bar{\mathcal{E}}_\alpha$ is given by

$$\begin{aligned} u(\bar{\mathcal{E}}_\alpha) &= \frac{1}{3}\text{tr}[T^\dagger_{\bar{\mathcal{E}},\alpha} T_{\bar{\mathcal{E}},\alpha}] \\ &= \sin\left(\frac{\pi\alpha}{2}\right)^4 + \frac{1}{6}\sin(\pi\alpha)^2 \\ &= \frac{1}{6}\sin\left(\frac{\pi\alpha}{2}\right)^2 (5 - \cos(\pi\alpha)). \end{aligned} \tag{D14}$$

This completes the proof.

### 2. Analytical form for marginal unitarities of $\text{CNOT}^\alpha_{AB}$ isometry

*Lemma D.2.* For the isometry $\mathcal{V}(\rho)_\alpha := \text{CNOT}^\alpha_{AB}(\rho \otimes |0\rangle\langle 0|)$ where $0 \leqslant \alpha \leqslant 1$, we define the marginals $\mathcal{E}_\alpha(\rho) := \text{tr}_B[\mathcal{V}(\rho)_\alpha]$ and $\bar{\mathcal{E}}_\alpha(\rho) := \text{tr}_A[\mathcal{V}(\rho)_\alpha]$. The unitarities of each marginal are

$$u(\mathcal{E}_\alpha) = 1 - \frac{2s}{3} \tag{D15}$$

and

$$u(\bar{\mathcal{E}}_\alpha) = \frac{s}{3} \tag{D16}$$

respectively, where $s = \sin^2(\frac{\pi\alpha}{2})$.

If we consider the sum of the marginals from Lemma E.2 we have

$$u(\mathcal{E}_\alpha) + u(\bar{\mathcal{E}}_\alpha) = 1 - \frac{s}{3} \tag{D17}$$

with $0 \leqslant s \leqslant 1$.

*Proof.* (of Lemma E.2) The proof follows in a similar way to the SWAP$^\alpha$ case. For the CNOT$_{AB}$ channel we use the notation CNOT$_{AB}(\rho) = U\rho U^\dagger$, to clarify that we mean the unitary matrix $U$ itself. We can diagonalise $U$ with respect to the computational basis by applying a Hadamard transform $H = (Z+X)/\sqrt{2}$ on the target qubit before and after such that the sandwiched unitary is the controlled phase gate,

$$\begin{aligned}U &= \tfrac{1}{2}(\mathbb{1}\otimes\mathbb{1} + Z\otimes\mathbb{1} + \mathbb{1}\otimes X - Z\otimes X),\\ &= \tfrac{1}{2}(\mathbb{1}\otimes H\mathbb{1}H + Z\otimes H\mathbb{1}H + \mathbb{1}\otimes HZH - Z\otimes HZH),\\ &= (\mathbb{1}\otimes H)\tfrac{1}{2}(\mathbb{1}\otimes\mathbb{1} + Z\otimes\mathbb{1} + \mathbb{1}\otimes Z - Z\otimes Z)(\mathbb{1}\otimes H),\\ &= (\mathbb{1}\otimes H)(|00\rangle\langle 00| + |01\rangle\langle 01| + |10\rangle\langle 10| - |11\rangle\langle 11|)\\ &\quad\times(\mathbb{1}\otimes H),\\ &= (\mathbb{1}\otimes H)(|00\rangle\langle 00| + |01\rangle\langle 01| + |10\rangle\langle 10| + e^{i\pi}|11\rangle\langle 11|)\\ &\quad\times(\mathbb{1}\otimes H).\end{aligned} \tag{D18}$$

Therefore we have

$$\begin{aligned}U^\alpha &= (\mathbb{1}\otimes H)(|00\rangle\langle 00| + |01\rangle\langle 01| + |10\rangle\langle 10| + e^{i\pi\alpha}|11\rangle\\ &\quad\times\langle 11|)(\mathbb{1}\otimes H),\\ &= |0\rangle\langle 0|\otimes\mathbb{1} + \tfrac{1}{2}(1+e^{i\pi\alpha})(|1\rangle\langle 1|\otimes\mathbb{1}) + \tfrac{1}{2}(1-e^{i\pi\alpha})\\ &\quad\times(|1\rangle\langle 1|\otimes X).\end{aligned} \tag{D19}$$

From the isometry definition we have $\mathcal{V}(\rho)_\alpha = U^\alpha\rho\otimes|0\rangle\langle 0|(U^\alpha)^\dagger$, substituting in the definition of $U^\alpha$ we can show that the unital block $T$ for the 1 qubit channels $\mathcal{E}_\alpha$ and $\bar{\mathcal{E}}_\alpha$ will be

$$T_{\mathcal{E},\alpha} = \begin{array}{c} \\ \langle X/\sqrt{2}| \\ \langle Y/\sqrt{2}| \\ \langle Z/\sqrt{2}| \end{array}\begin{array}{c} \begin{array}{ccc} |X/\sqrt{2}\rangle & |Y/\sqrt{2}\rangle & |Z/\sqrt{2}\rangle \end{array} \\ \begin{pmatrix} \cos^2\left(\frac{\pi\alpha}{2}\right) & \frac{1}{2}\sin(\pi\alpha) & 0 \\ -\frac{1}{2}\sin(\pi\alpha) & \cos^2\left(\frac{\pi\alpha}{2}\right) & 0 \\ 0 & 0 & 1 \end{pmatrix} \end{array}, \tag{D20}$$

and

$$T_{\bar{\mathcal{E}},\alpha} = \begin{array}{c} \\ \langle X/\sqrt{2}| \\ \langle Y/\sqrt{2}| \\ \langle Z/\sqrt{2}| \end{array}\begin{array}{c} \begin{array}{ccc} |X/\sqrt{2}\rangle & |Y/\sqrt{2}\rangle & |Z/\sqrt{2}\rangle \end{array} \\ \begin{pmatrix} 0 & 0 & 0 \\ 0 & 0 & 0 \\ 0 & \frac{1}{2}\sin(\pi\alpha) & \sin^2\left(\frac{\pi\alpha}{2}\right) \end{pmatrix} \end{array}, \tag{D21}$$

respectively. Therefore, with some multiplication, the unitarity of $\mathcal{E}_\alpha$ is given by $u(\mathcal{E}_\alpha) = 1 - \frac{2}{3}\sin^2(\frac{\alpha\pi}{2})$ and the unitarity of $\bar{\mathcal{E}}_\alpha$ is given by $u(\bar{\mathcal{E}}_\alpha) = \frac{1}{3}\sin^2(\frac{\alpha\pi}{2})$. This completes the proof. ■

### 3. Analytical form for marginal unitarities of CNOT$^\alpha_{BA}\circ$CNOT$_{AB}$ isometry

*Lemma D.3.* For the isometry $\mathcal{V}(\rho)_\alpha := \text{CNOT}^\alpha_{BA}\circ\text{CNOT}_{AB}(\rho\otimes|0\rangle\langle 0|)$ where $0\leqslant\alpha\leqslant 1$, we define the marginals $\mathcal{E}_\alpha(\rho) := \text{tr}_B[\mathcal{V}(\rho)_\alpha]$ and $\bar{\mathcal{E}}_\alpha(\rho) := \text{tr}_A[\mathcal{V}(\rho)_\alpha]$. The unitarities of each marginal are

$$u(\mathcal{E}_\alpha) = \tfrac{1}{3}(1-s) \tag{D22}$$

and

$$u(\bar{\mathcal{E}}_\alpha) = 1 - \tfrac{2}{3}(1-s) \tag{D23}$$

respectively, where $s = \sin^2(\frac{\pi\alpha}{2})$.

If we consider the sum of the marginals from Lemma E.3 we have

$$u(\mathcal{E}_\alpha) + u(\bar{\mathcal{E}}_\alpha) = 1 - \tfrac{1}{3}(1-s) \tag{D24}$$

with $0\leqslant s\leqslant 1$.

*Proof.* (of Lemma E.3) Proof follows in the same way as the previous two lemmas. From the previous lemma we can write the unitary matrix for the channel CNOT$_{BA}(\rho) := U_{BA}\rho U^\dagger_{BA}$ as

$$\begin{aligned}U_{BA} &= (H\otimes\mathbb{1})(|00\rangle\langle 00| + |01\rangle\langle 01| + |10\rangle\langle 10| + e^{i\pi}|11\rangle\\ &\quad\times\langle 11|)(H\otimes\mathbb{1}),\end{aligned} \tag{D25}$$

and therefore

$$\begin{aligned}U^\alpha_{BA} &= (H\otimes\mathbb{1})(|00\rangle\langle 00| + |01\rangle\langle 01| + |10\rangle\langle 10| + e^{i\pi\alpha}|11\rangle\\ &\quad\times\langle 11|)(H\otimes\mathbb{1}),\\ &= \mathbb{1}\otimes|0\rangle\langle 0| + \tfrac{1}{2}(1+e^{i\pi\alpha})(\mathbb{1}\otimes|1\rangle\langle 1|) + \tfrac{1}{2}(1-e^{i\pi\alpha})\\ &\quad\times(X\otimes|1\rangle\langle 1|).\end{aligned} \tag{D26}$$

The unitary matrix for the channel CNOT$_{AB}(\rho) := U_{AB}\rho U^\dagger_{AB}$ is given in the Pauli basis as

$$U_{AB} = \tfrac{1}{2}(\mathbb{1}\otimes\mathbb{1} + Z\otimes\mathbb{1} + \mathbb{1}\otimes X - Z\otimes X), \tag{D27}$$

therefore from the isometry definition $\mathcal{V}(\rho)_\alpha = U^\alpha_{BA}U_{AB}\rho\otimes|0\rangle\langle 0|U^\dagger_{AB}(U^\alpha_{BA})^\dagger$ we can show that the unital block $T$ for the 1 qubit channels $\mathcal{E}_\alpha$ and $\bar{\mathcal{E}}_\alpha$ will be

$$T_{\mathcal{E},\alpha} = \begin{array}{c} \\ \langle X/\sqrt{2}| \\ \langle Y/\sqrt{2}| \\ \langle Z/\sqrt{2}| \end{array}\begin{array}{c} \begin{array}{ccc} |X/\sqrt{2}\rangle & |Y/\sqrt{2}\rangle & |Z/\sqrt{2}\rangle \end{array} \\ \begin{pmatrix} 0 & 0 & 0 \\ 0 & 0 & 0 \\ 0 & -\frac{1}{2}\sin(\pi\alpha) & \cos^2\left(\frac{\pi\alpha}{2}\right) \end{pmatrix} \end{array}, \tag{D28}$$

and

$$T_{\bar{\mathcal{E}},\alpha} = \begin{array}{c} \\ \langle X/\sqrt{2}| \\ \langle Y/\sqrt{2}| \\ \langle Z/\sqrt{2}| \end{array}\begin{array}{c} \begin{array}{ccc} |X/\sqrt{2}\rangle & |Y/\sqrt{2}\rangle & |Z/\sqrt{2}\rangle \end{array} \\ \begin{pmatrix} \sin^2\left(\frac{\pi\alpha}{2}\right) & -\frac{1}{2}\sin(\pi\alpha) & 0 \\ \frac{1}{2}\sin(\pi\alpha) & \sin^2\left(\frac{\pi\alpha}{2}\right) & 0 \\ 0 & 0 & 1 \end{pmatrix} \end{array}, \tag{D29}$$

respectively. Therefore, with some multiplication, the unitarity of $\mathcal{E}_\alpha$ is given by $u(\mathcal{E}_\alpha) = \frac{1}{3}\cos^2(\frac{\alpha\pi}{2})$ and the unitarity of $\bar{\mathcal{E}}_\alpha$ is given by $u(\bar{\mathcal{E}}_\alpha) = 1 - \frac{2}{3}\cos^2(\frac{\alpha\pi}{2})$. This completes the proof. ■

## APPENDIX E: SPAM ROBUST ESTIMATION THROUGH INTERLEAVED RB

### 1. Interleaved unitarity protocol for $(\mathcal{E}, \bar{\mathcal{E}})$ without noise

We now give a sketch of the proof for Protocol 1. Define the elements of the Clifford group on qubit $A$ to be $\{\mathcal{U}_{A,i}\}$. We define channel induced by averaging over many Clifford unitaries as

$$\mathcal{U}_A := \frac{1}{N}\sum_i^N \mathcal{C}_{A,i}. \tag{E1}$$

In the case $\Lambda = \Lambda_C = id$, the circuit diagram representation of Protocol 1 is

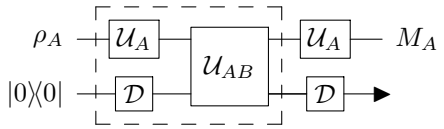


(E2)

where ◀ indicates the channel preparing $|0\rangle\langle 0|$ and ▶ the trace operation. As ▶◀$= \mathcal{D}$, the circuit reduces to

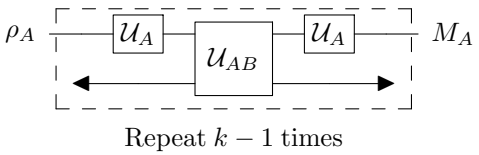


(E3)

which further reduces to

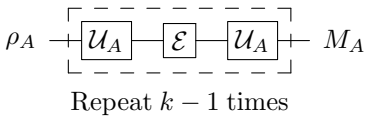


(E4)

Which is exactly the right form for the circuit to estimate $u(\mathcal{E})$. The decay parameter $e_1$ in Protocol 1 is exactly $u(\mathcal{E})$ in this idealized case.

The protocol to estimate $u(\bar{\mathcal{E}})$ is the same as for $u(\mathcal{E})$ replacing $\mathcal{U}_{AB}$ with $SWAP \circ \mathcal{U}_{AB}$. This follows from the fact that

$$\begin{aligned}\bar{\mathcal{E}}(\rho) &:= \mathrm{tr}_A \circ \mathcal{U}_{AB}(\rho \otimes |0\rangle\langle 0|) \\ &= \mathrm{tr}_B \circ SWAP \circ \mathcal{U}_{AB}(\rho \otimes |0\rangle\langle 0|),\end{aligned} \tag{E5}$$

or as a circuit diagram

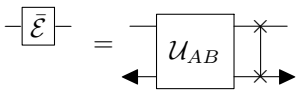


(E6)

where we implicitly assume $d_A = d_B$, which is appropriate in this two qubit case.

### 2. Efficient implementation of protocols

In the experiments for the SPAM robust CUP set, we perform an *efficient* unitarity RB protocol, as introduced in [36]. The protocol allows for rigorous bounds on the variance in the associated decay curve, and therefore the value of unitarity extracted. We summarize the efficient unitarity RB protocol applied to our scheme here, where we consider $\mathcal{E}$ as a black box single qubit channel whose implementation is detailed in Appendix E 1.

Protocol 2: Efficient interleaved unitarity RB for $\mathcal{E}$.

1. **Select** a random sequence, $\mathcal{U}_{\mathbf{k}} := \mathcal{U}_k \circ \mathcal{E} \circ \mathcal{U}_{k-1} \circ \mathcal{E} \circ ... \circ \mathcal{U}_2 \circ \mathcal{E} \circ \mathcal{U}_1$, of random Clifford gates interleaved with target channel $\mathcal{E}$.
2. **Prepare** the system in the state $\rho_{\pm,i} := \frac{1}{d}(\mathbb{1} \pm P_i)$ for all nonidentity elements $P_i$, of the Pauli group $P \neq \mathbb{1}$. In the single qubit input and output case, the states $\rho_{\pm,i}$ are pure states given by $\rho_{\pm,i} = \{|+\rangle, |-\rangle, |+i\rangle, |-i\rangle, |0\rangle, |1\rangle\}$.
3. **Estimate** the average purity of the sequence across all possible traceless input and output Pauli: $q_{\mathbf{k}} = \frac{1}{d^2-1}\sum_{i,j}^{d^2-1}(\mathrm{tr}[P_j\, \mathcal{C}_{\mathbf{k}}(\rho_{+,i})] - \mathrm{tr}[P_j\, \mathcal{C}_{\mathbf{k}}(\rho_{-,i})])^2$.
4. **Repeat 1, 2, and 3** for $N_k$ random sequences of length $k$, finding the average estimation $\mathbb{E}[q_{\mathbf{k}}] := \frac{1}{N_k}\sum_{\mathbf{k}}^{\mathbf{N_k}} q_{\mathbf{k}}$.
5. **Repeat 1, 2, 3, and 4** increasing the length of the sequence, e.g., $k = k + 1$.
6. **Fit** the data with $\mathbb{E}[q_{\mathbf{k}}] = c_1 s^{k-1}$, to find $s$ the estimated value of $u(\mathcal{E})$.

### 3. Interleaved unitarity protocol for $(\mathcal{E}, \bar{\mathcal{E}})$ with noise

In this section we set out the minimum assumptions required to produce interleaved unitarity RB circuits, where all operations are assumed to be noisy. We then show how this effects the estimation of CUP sets. For channels, states, functions, any $X$, we write the noisy version $X_N$.

For a two qubit system when we implement any gate or mid-circuit measurement, the noise associated with the process may effect the whole device. Therefore we should model errors as bipartite quantum channels. We make two simplifying assumptions about these errors. Firstly, we consider the noise to be fixed across the Clifford group gateset, such that $\Lambda_{\mathcal{C},i} = \Lambda_{\mathcal{C}}$ for all $\mathcal{U}_i$. For example, $\mathcal{U}_{i,N} = \Lambda_{\mathcal{C}} \circ \mathcal{U}_i \otimes id_B$. Secondly, we assume the reset of a qubit is perfectly incoherent, but potentially noisy. Therefore the total channel can be written as $\mathcal{D}_{B,N} = \Lambda_{\mathcal{D}} \circ id_A \otimes \mathcal{D}_B$, with a general bipartite error channel $\Lambda_{\mathcal{D}}$.

A direct consequence of these two assumptions is that we can write the noisy version of the summation of Clifford unitaries $\mathcal{U}_{A,N}$ and the reset operation as

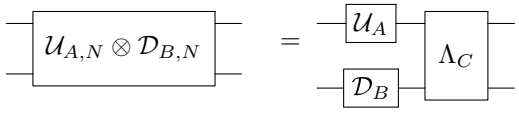


(E7)

where $\Lambda_C$ is an error channel associated with the operations together. Putting this together with a noisy version of the interleaved unitary $\mathcal{U}_{AB,N} = \mathcal{U}_{AB} \circ \Lambda_{AB}$ we can write a noisy version of the circuit for Protocol 1:

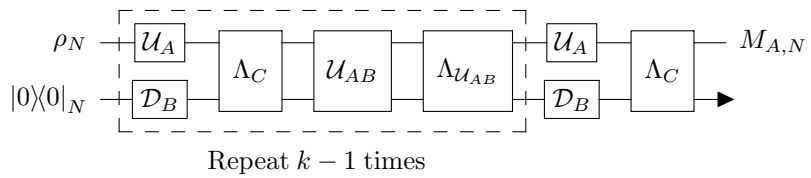


(E8)

Further we can write the reset operations as trace and preparation operations in our notation and absorb the initial and final error channels as SPAM errors in the $A$ subsystem. This leaves us with

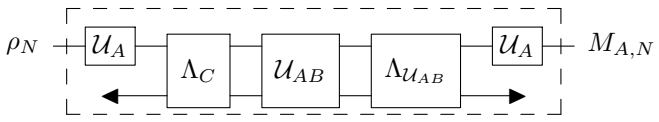


(E9)

As the protocol is SPAM robust, we get an estimation of the unitarity $u(\mathcal{E}_N)$ of the channel $\mathcal{E}_N(\rho) := tr_B \circ \Lambda_{AB} \circ \mathcal{U}_{AB} \circ \Lambda_C(\rho \otimes |0\rangle\langle 0|)$.

When we implement the protocol for $\bar{\mathcal{E}}$ we will have an additional required operation, *SWAP*, and the noise associated with it. We can write the noisy version of this in full generality, by including it with the preceding defined unitary $\mathcal{U}_{AB}$. For example, $SWAP_N \circ \mathcal{U}_{AB,N} := \Lambda_{S,AB} \circ SWAP \circ \mathcal{U}_{AB}$. This leads to a noisy circuit of the form

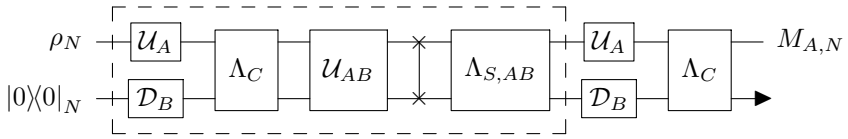


(E10)

Finally, absorbing the initial and final error channels as SPAM errors in the $A$ subsystem leaves us with

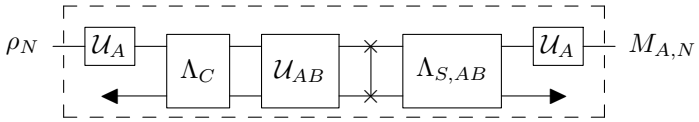


(E11)

Giving an exact estimation of the unitarity $u(\bar{\mathcal{E}}_N)$ for the channel $\bar{\mathcal{E}}_N(\rho) := tr_A \circ \Lambda_{S,AB} \circ \mathcal{U}_{AB} \circ \Lambda_C(\rho \otimes |0\rangle\langle 0|)$.


[1] W. K. Wootters and W. H. Zurek, A single quantum cannot be cloned, Nature (London) **299**, 802 (1982).

[2] H. P. Yuen, Amplification of quantum states and noiseless photon amplifiers, Phys. Lett. A **113**, 405 (1986).

[3] H. Barnum, J. Barrett, M. Leifer, and A. Wilce, Generalized no-broadcasting theorem, Phys. Rev. Lett. **99**, 240501 (2007).

[4] H. Barnum, C. M. Caves, C. A. Fuchs, R. Jozsa, and B. Schumacher, Noncommuting mixed states cannot be broadcast, Phys. Rev. Lett. **76**, 2818 (1996).

[5] D. Kretschmann, D. Schlingemann, and R. F. Werner, The information-disturbance tradeoff and the continuity of Stinespring's representation, IEEE Trans. Inf. Theory **54**, 1708 (2008).

[6] T. Heinosaari, T. Miyadera, and M. Ziman, An invitation to quantum incompatibility, J. Phys. A: Math. Theor. **49**, 123001 (2016).

[7] A. Bluhm, A. Jenčová, and I. Nechita, Incompatibility in general probabilistic theories, generalized spectrahedra, and tensor norms, Commun. Math. Phys. **393**, 1125 (2022).

[8] A. Jenčová, Incompatible measurements in a class of general probabilistic theories, Phys. Rev. A **98**, 012133 (2018).

[9] B. Hensen, H. Bernien, A. E. Dréau, A. Reiserer, N. Kalb, M. S. Blok, J. Ruitenberg, R. F. Vermeulen, R. N. Schouten, C. Abellán *et al.*, Loophole-free Bell inequality violation using electron spins separated by 1.3 kilometres, Nature (London) **526**, 682 (2015).

[10] M. Giustina, M. A. Versteegh, S. Wengerowsky, J. Handsteiner, A. Hochrainer, K. Phelan, F. Steinlechner, J. Kofler, J.-Å. Larsson, C. Abellán *et al.*, Significant-loophole-free test of Bell's theorem with entangled photons, Phys. Rev. Lett. **115**, 250401 (2015).

[11] L. K. Shalm, E. Meyer-Scott, B. G. Christensen, P. Bierhorst, M. A. Wayne, M. J. Stevens, T. Gerrits, S. Glancy, D. R. Hamel, M. S. Allman *et al.*, Strong loophole-free test of local realism, Phys. Rev. Lett. **115**, 250402 (2015).

[12] J. R. Samal, A. K. Pati, and A. Kumar, Experimental test of the quantum no-hiding theorem, Phys. Rev. Lett. **106**, 080401 (2011).

[13] H. Gao, L. Xiao, K. Wang, D. Qu, Q. Lin, and P. Xue, Experimental verification of trade-off relation for coherence and disturbance, New J. Phys. **24**, 073011 (2022).

[14] J. Preskill, Quantum computing in the NISQ era and beyond, Quantum **2**, 79 (2018).

[15] H. Bombín, Single-shot fault-tolerant quantum error correction, Phys. Rev. X **5**, 031043 (2015).

[16] Y. Suzuki, S. Endo, K. Fujii, and Y. Tokunaga, Quantum error mitigation as a universal error reduction technique: Applications from the NISQ to the fault-tolerant quantum computing eras, PRX Quantum **3**, 010345 (2022).

[17] M. A. Nielsen and I. Chuang, *Quantum Computation and Quantum Information* (Cambridge University Press, Cambridge, 2002).

[18] S. Sadana, L. Maccone, and U. Sinha, Testing quantum foundations with quantum computers, Phys. Rev. Res. **4**, L022001 (2022).

[19] C. Carmeli, T. Heinosaari, T. Miyadera, and A. Toigo, Witnessing incompatibility of quantum channels, J. Math. Phys. **60**, 122202 (2019).

[20] C. Carmeli, T. Heinosaari, and A. Toigo, Quantum incompatibility witnesses, Phys. Rev. Lett. **122**, 130402 (2019).

[21] M. Girard, M. Plávala, and J. Sikora, Jordan products of quantum channels and their compatibility, Nat. Commun. **12**, 2129 (2021).

[22] Q.-H. Zhang and I. Nechita, A fisher information-based incompatibility criterion for quantum channels, Entropy **24**, 805 (2022).

[23] D. Kretschmann, D. Schlingemann, and R. F. Werner, A continuity theorem for Stinespring's dilation, J. Funct. Anal. **255**, 1889 (2008).

[24] E. Haapasalo, Robustness of incompatibility for quantum devices, J. Phys. A: Math. Theor. **48**, 255303 (2015).

[25] S. Designolle, M. Farkas, and J. Kaniewski, Incompatibility robustness of quantum measurements: A unified framework, New J. Phys. **21**, 113053 (2019).

[26] S. L. Braunstein and A. K. Pati, Quantum information cannot be completely hidden in correlations: Implications for the black-hole information paradox, Phys. Rev. Lett. **98**, 080502 (2007).

[27] S. B. Giddings, The black hole information paradox, arXiv:hep-th/9508151.

[28] J. Maldacena, Black holes and quantum information, Nat. Rev. Phys. **2**, 123 (2020).

[29] K. Modi, A. K. Pati, A. Sen(De), and U. Sen, Masking quantum information is impossible, Phys. Rev. Lett. **120**, 230501 (2018).

[30] H. Zhu, Hiding and masking quantum information in complex and real quantum mechanics, Phys. Rev. Res. **3**, 033176 (2021).

[31] A. Kumar Pati and S. L. Braunstein, Impossibility of deleting an unknown quantum state, Nature (London) **404**, 164 (2000).

[32] A. R. Kalra, N. Gupta, B. K. Behera, S. Prakash, and P. K. Panigrahi, Demonstration of the no-hiding theorem on the 5-qubit IBM quantum computer in a category-theoretic framework, Quantum Info. Proc. **18**, 1 (2019).

[33] J. Eisert, D. Hangleiter, N. Walk, I. Roth, D. Markham, R. Parekh, U. Chabaud, and E. Kashefi, Quantum certification and benchmarking, Nat. Rev. Phys. **2**, 382 (2020).

[34] M. Kliesch and I. Roth, Theory of quantum system certification, PRX Quantum **2**, 010201 (2021).

[35] J. Wallman, C. Granade, R. Harper, and S. T. Flammia, Estimating the coherence of noise, New J. Phys. **17**, 113020 (2015).

[36] B. Dirkse, J. Helsen, and S. Wehner, Efficient unitarity randomized benchmarking of few-qubit clifford gates, Phys. Rev. A **99**, 012315 (2019).

[37] A. Carignan-Dugas, J. J. Wallman, and J. Emerson, Bounding the average gate fidelity of composite channels using the unitarity, New J. Phys. **21**, 053016 (2019).

[38] In quantum theory this is $\gamma(\rho) := \mathrm{tr}[\rho^2]$ for any state $\rho$.

[39] G. Chiribella and R. W. Spekkens, *Quantum Theory: Informational Foundations and Foils* (Springer, New York, 2016).

[40] M. Plávala, General probabilistic theories: An introduction, Phys. Rep. **1033**, 1 (2023).

[41] H. Barnum, J. Barrett, M. Leifer, and A. Wilce, Cloning and broadcasting in generic probabilistic theories, arXiv:quant-ph/0611295.

[42] M. Horodecki, P. Horodecki, and R. Horodecki, General teleportation channel, singlet fraction, and quasidistillation, Phys. Rev. A **60**, 1888 (1999).

[43] E. Knill, D. Leibfried, R. Reichle, J. Britton, R. B. Blakestad, J. D. Jost, C. Langer, R. Ozeri, S. Seidelin, and D. J. Wineland, Randomized benchmarking of quantum gates, Phys. Rev. A **77**, 012307 (2008).

[44] H. Buhrman, R. Cleve, J. Watrous, and R. De Wolf, Quantum fingerprinting, Phys. Rev. Lett. **87**, 167902 (2001).

[45] E. Magesan, J. M. Gambetta, B. R. Johnson, C. A. Ryan, J. M. Chow, S. T. Merkel, M. P. Da Silva, G. A. Keefe, M. B. Rothwell, T. A. Ohki *et al.*, Efficient measurement of quantum gate error by interleaved randomized benchmarking, Phys. Rev. Lett. **109**, 080505 (2012).

[46] J. Helsen, F. Battistel, and B. M. Terhal, Spectral quantum tomography, npj Quantum Inf. **5**, 1 (2019).

[47] K. Korzekwa, S. Czachórski, Z. Puchała, and K. Życzkowski, Coherifying quantum channels, New J. Phys. **20**, 043028 (2018).

[48] More precisely a pure state is an extremal point in the set of all states, such as $|\psi\rangle\langle\psi|$ in quantum theory, while a mixed state is obtained from probabilistic mixtures of pure states.

[49] M. Müller-Lennert, F. Dupuis, O. Szehr, S. Fehr, and M. Tomamichel, On quantum Rényi entropies: A new generalization and some properties, J. Math. Phys. **54**, 122203 (2013).

[50] C. Cîrstoiu, K. Korzekwa, and D. Jennings, Robustness of Noether's principle: Maximal disconnects between conservation laws and symmetries in quantum theory, Phys. Rev. X **10**, 041035 (2020).

[51] A. Nayak and P. Sen, Invertible quantum operations and perfect encryption of quantum states, arXiv:quant-ph/0605041.

[52] C. Heunen and R. Kaarsgaard, Bennett and Stinespring, together at last, arXiv:2102.08711.

[53] C. H. Bennett, Logical reversibility of computation, IBM J. Res. Dev. **17**, 525 (1973).

[54] J. Watrous, *The Theory of Quantum Information* (Cambridge University Press, Cambridge, 2018), p. 23.

[55] S. Aaronson, D. Grier, and L. Schaeffer, The classification of reversible bit operations, arXiv:1504.05155.

[56] H. B. Axelsen and R. Glück, What do reversible programs compute? in *International Conference on Foundations of Software Science and Computational Structures* (Springer, New York, 2011), pp. 42–56.

[57] C. E. Shannon, Communication theory of secrecy systems, Bell Syst. Tech. J. **28**, 656 (1949).

[58] J. J. Wallman and J. Emerson, Noise tailoring for scalable quantum computation via randomized compiling, Phys. Rev. A **94**, 052325 (2016).

[59] J. J. Wallman, Bounding experimental quantum error rates relative to fault-tolerant thresholds, arXiv:1511.00727.

[60] F. Vatan and C. Williams, Optimal quantum circuits for general two-qubit gates, Phys. Rev. A **69**, 032315 (2004).

[61] K. Dubovitskii and Y. Makhlin, Partial randomized benchmarking, Sci. Rep. **12**, 10129 (2022).

[62] V. Scarani, S. Iblisdir, N. Gisin, and A. Acin, Quantum cloning, Rev. Mod. Phys. **77**, 1225 (2005).

[63] H. Fan, Y.-N. Wang, L. Jing, J.-D. Yue, H.-D. Shi, Y.-L. Zhang, and L.-Z. Mu, Quantum cloning machines and the applications, Phys. Rep. **544**, 241 (2014).

[64] A.-L. Hashagen, Universal asymmetric quantum cloning revisited, Quantum Info. Comput. **17**, 747 (2017).

[65] M. Jiang and S. Yu, Extremal asymmetric universal cloning machines, J. Math. Phys. **51**, 052306 (2010).

[66] D. Bruß, D. P. DiVincenzo, A. Ekert, C. A. Fuchs, C. Macchiavello, and J. A. Smolin, Optimal universal and state-dependent quantum cloning, Phys. Rev. A **57**, 2368 (1998).

[67] N. Gisin and S. Massar, Optimal quantum cloning machines, Phys. Rev. Lett. **79**, 2153 (1997).

[68] S. L. Braunstein, V. Bužek, and M. Hillery, Quantum-information distributors: Quantum network for symmetric and asymmetric cloning in arbitrary dimension and continuous limit, Phys. Rev. A **63**, 052313 (2001).

[69] M. M. Wolf and D. Perez-Garcia, The inverse eigenvalue problem for quantum channels, arXiv:1005.4545.

[70] A. Elben, S. T. Flammia, H.-Y. Huang, R. Kueng, J. Preskill, B. Vermersch, and P. Zoller, The randomized measurement toolbox, Nat. Rev. Phys. **5**, 9 (2022).

[71] D. Stilck França and R. Garcia-Patron, Limitations of optimization algorithms on noisy quantum devices, Nat. Phys. **17**, 1221 (2021).

[72] D. Aharonov, X. Gao, Z. Landau, Y. Liu, and U. Vazirani, A polynomial-time classical algorithm for noisy random circuit sampling, in *Proceedings of the 55th Annual ACM Symposium on Theory of Computing, June 2023*, STOC 2023 (ACM, New York, 2023), pp. 945–957.

[73] G. Chiribella, G. M. D'Ariano, and P. Perinotti, Probabilistic theories with purification, Phys. Rev. A **81**, 062348 (2010).

[74] P. Janotta and H. Hinrichsen, Generalized probability theories: what determines the structure of quantum theory? J. Phys. A: Math. Theor. **47**, 323001 (2014).

[75] J. Barrett, Information processing in generalized probabilistic theories, Phys. Rev. A **75**, 032304 (2007).

[76] L. Hardy, Quantum theory from five reasonable axioms, arXiv:quant-ph/0101012.

[77] T. Heinosaari and T. Miyadera, Incompatibility of quantum channels, J. Phys. A: Math. Theor. **50**, 135302 (2017).

[78] M. A. Man'ko and V. I. Man'ko, Deformed subadditivity condition for qudit states and hybrid positive maps, J. Russ. Laser Res. **35**, 509 (2014).

[79] A. S. Holevo, Complementary channels and the additivity problem, Theory Probab. Appl. **51**, 92 (2007).

[80] R. A. Horn and C. R. Johnson, *Matrix Analysis*, 2nd ed. (Cambridge University Press, Cambridge, 2012).

[81] P. Appel, M. Huber, and C. Klöckl, Monogamy of correlations and entropy inequalities in the Bloch picture, J. Phys. Commun. **4**, 025009 (2020).

[82] R. Bhatia, *Matrix Analysis*, Vol. 169 (Springer Science & Business Media, New York, 2013).

[83] M. Girling, C. Cîrstoiu, and D. Jennings, Estimation of correlations and nonseparability in quantum channels via unitarity benchmarking, Phys. Rev. Res. **4**, 023041 (2022).

[84] I. Bengtsson and K. Życzkowski, *Geometry of Quantum States: An Introduction to Quantum Entanglement* (Cambridge University Press, Cambridge, 2017).

[85] H. Fan, V. Roychowdhury, and T. Szkopek, Optimal two-qubit quantum circuits using exchange interactions, Phys. Rev. A **72**, 052323 (2005).